Rapid and Body Weight-Independent Improvement of Endothelial and High-Density Lipoprotein Function After Roux-en-Y Gastric Bypass: Role of Glucagon-Like Peptide-1

Osto, Elena ; Doytcheva, Petia ; Corteville, Caroline ; Bueter, Marco ; Dörig, Claudia ; Stivala, Simona ; Buhmann, Helena ; Colin, Sophie ; Rohrer, Lucia ; Hasballa, Reda ; Tailleux, Anne ; Wolfrum, Christian ; Tona, Francesco ; Manz, Jasmin ; Vetter, Diana ; Spliethoff, Kerstin ; Vanhoutte, Paul M ; Landmesser, Ulf ; Pattou, Francois ; Staels, Bart ; Matter, Christian M ; Lutz, Thomas A ; Lüscher, Thomas F

Abstract: BACKGROUND Roux-en-Y gastric bypass (RYGB) reduces body weight and cardiovascular mortality in morbidly obese patients. Glucagon-like peptide-1 (GLP-1) seems to mediate the metabolic benefits of RYGB partly in a weight loss-independent manner. The present study investigated in rats and patients whether obesity-induced endothelial and high-density lipoprotein (HDL) dysfunction is rapidly improved after RYGB via a GLP-1-dependent mechanism. METHODS AND RESULTS Eight days after RYGB in diet-induced obese rats, higher plasma levels of bile acids and GLP-1 were associated with improved endothelium-dependent relaxation compared with sham-operated controls fed ad libitum and sham-operated rats that were weight matched to those undergoing RYGB. Compared with the sham-operated rats, RYGB improved nitric oxide (NO) bioavailability resulting from higher endothelial Akt/NO synthase activation, reduced c-Jun amino terminal kinase phosphorylation, and decreased oxidative stress. The protective effects of RYGB were prevented by the GLP-1 receptor antagonist exendin9-39 (10 $g \cdot kg(-1) \cdot h(-1)$). Furthermore, in patients and rats, RYGB rapidly reversed HDL dysfunction and restored the endothelium-protective properties of the lipoprotein, including endothelial NO synthase activation, NO production, and anti-inflammatory, antiapoptotic, and antioxidant effects. Finally, RYGB restored HDL-mediated cholesterol efflux capacity. To demonstrate the role of increased GLP-1 signaling, sham-operated control rats were treated for 8 days with the GLP-1 analog liraglutide (0.2 mg/kg twice daily), which restored NO bioavailability and improved endothelium-dependent relaxations and HDL endothelium-protective properties, mimicking the effects of RYGB. CONCLUSIONS RYGB rapidly reverses obesity-induced endothelial dysfunction and restores the endothelium-protective properties of HDL via a GLP-1-mediated mechanism. The present translational findings in rats and patients unmask novel, weight-independent mechanisms of cardiovascular protection in morbid obesity.

DOI: https://doi.org/10.1161/CIRCULATIONAHA.114.011791

Osto, Elena; Doytcheva, Petia; Corteville, Caroline; Bueter, Marco; Dörig, Claudia; Stivala, Simona; Buhmann, Helena; Colin, Sophie; Rohrer, Lucia; Hasballa, Reda; Tailleux, Anne; Wolfrum, Christian; Tona, Francesco; Manz, Jasmin; Vetter, Diana; Spliethoff, Kerstin; Vanhoutte, Paul M; Landmesser, Ulf; Pattou, Francois; Staels, Bart; Matter, Christian M; Lutz, Thomas A; Lüscher, Thomas F (2015). Rapid and Body Weight-Independent Improvement of Endothelial and High-Density Lipoprotein Function After Roux-en-Y Gastric Bypass: Role of Glucagon-Like Peptide-1. Circulation, 131(10):871-881.
DOI: https://doi.org/10.1161/CIRCULATIONAHA.114.011791

CIRCULATIONAHA/2014/011791 R1

November 23rd, 2014

Rapid and body weight-independent improvement of endothelial and HDL function after Roux-en-Y gastric bypass: role of glucagon-like peptide-1

°Elena Osto, MD, PhD[1, *]; Petia Doytcheva, Msc[1,2*];Caroline Corteville, MD[2]; Marco Bueter, MD, PhD[3], Claudia Dörig, Msc[2], Simona Stivala, PhD[1],Helena Buhmann, MD[2], Sophie Colin, PhD[4], Lucia Rohrer, PhD[5]; Reda Hasballa Msc[5], Anne Tailleux, PhD[4], Christian Wolfrum PhD[6], .Francesco Tona, MD, PhD[7], Jasmin Manz Msc[1], Diana Vetter, MD[3], Kerstin Spliethoff DVM[2], Paul M. Vanhoutte MD, PhD[8], Ulf Landmesser, MD[1], Francois Pattou, MD, PhD[9], Bart Staels MD[4], Christian M. Matter, MD[1], Thomas A. Lutz DVM, PhD[2*], and Thomas F. Lüscher MD[1*].

1 Centre for Molecular Cardiology, University of Zurich and University Heart Center, Cardiology, University Hospital Zurich, Switzerland, 2Institute of Veterinary Physiology, University of Zurich, Switzerland, 3Department of Surgery, University Hospital Zurich, Switzerland, 4 Université Lille 2, INSERM UMR1011, EGID, Institut Pasteur de Lille, Lille, France , 5Institute of Clinical Chemistry, University Hospital Zurich, Switzerland,6 Department of Health Sciences and Technology, ETH Zurich, Switzerland, 7Department of Cardiac, Thoracic and Vascular Sciences, University of Padua, Italy ,8State Key Laboratory for Pharmaceutical Biotechnologies &Department of Pharmacology & Pharmacy, LKS Faculty of Medicine, The University of Hong Kong, 9Department of Endocrine Surgery, Lille University Hospital, France.

Running title: rapid effects of RYGB on endothelial and HDL function

Word count: 6993

Address for Correspondence °Elena Osto, M.D., Ph.D.

Centre for Molecular Cardiology

University of Zurich

Wagistrasse, 12

CH-8952 Schlieren, Switzerland

Tel: +41-44-635 6469

Fax: +41-44-635 6827

Email: elena.osto@uzh.ch

*These authors contributed equally.

Abstract

Background: Roux-en-Y gastric bypass (RYGB) reduces body weight and cardiovascular mortality in morbidly obese patients. Glucagon-like peptide-1 (GLP-1) seems to mediate the metabolic benefits of RYGB partly in a weight loss-independent manner. The present study investigated in rats and patients whether obesity-induced endothelial and HDL dysfunction are rapidly improved after RYGB via a GLP-1-dependent mechanism.

Methods and Results: Eight days after RYGB in diet-induced obese rats, higher plasma levels of bile acids and GLP-1 were associated with improved endothelium-dependent relaxation compared to sham-operated controls fed *ad libitum* and sham-operated rats that were weight-matched to those undergoing RYGB. Compared to sham-operated rats, RYGB improved nitric oxide (NO) bioavailability due to higher endothelial Akt/NO synthase activation, reduced JNK-phosphorylation and decreased oxidative stress. The protective effects of RYGB were prevented by the GLP-1 receptor antagonist exendin$_{9\text{-}39}$ (10ug/kg/h). Further, in patients and rats RYGB rapidly reversed HDL dysfunction and restored the endothelium-protective properties of the lipoprotein, including eNOS activation, NO production as well as anti-inflammatory, anti-apoptotic and anti-oxidant effects. Finally, RYGB restored HDL-mediated cholesterol efflux capacity. To demonstrate the role of increased GLP-1 signaling, sham-operated control rats were treated for eight days with the GLP-1 analog liraglutide (0.2 mg/kg twice daily), which restored NO bioavailability, improved endothelium-dependent relaxations and HDL endothelium-protective properties, mimicking the effects of RYGB.

Conclusions: RYGB rapidly reverses obesity-induced endothelial dysfunction and restores the endothelium-protective properties of HDL via a GLP-1-mediated mechanism. The present translational findings in rats and patients unmask novel, weight-independent mechanisms of cardiovascular protection in morbid obesity.

Introduction

Obesity is a worldwide health problem due to the associated increased morbidity and cardiovascular mortality[1]. Accompanying metabolic disorders such as insulin resistance, type 2 diabetes mellitus (T2DM) and risk factors such as dyslipidemia increase the disease risk linked to obesity. In particular, obesity induces endothelial dysfunction which precedes atherosclerosis, but also contributes to insulin resistance in tissues involved in glucose and lipid metabolism[2, 3]. Reduced nitric oxide (NO) bioavailability seems to be the primary defect that links obesity, insulin resistance and endothelial dysfunction[2, 3].

Furthermore, obesity and insulin resistance result in pro-atherogenic dyslipidemia[4] characterized by high low density lipoproteins (LDL) and triglyceride (TG) and low high-density lipoproteins (HDL) cholesterol plasma levels[1, 5]. Abnormal HDL remodeling and maturation have been reported in obese subjects with a HDL profile similar to that of subjects with established cardiovascular disease[5]. In addition, pathological situations associated with obesity, in particular T2DM[6] and coronary artery disease[7], impair the physiological protective properties of HDL, which preserves endothelial NO bioavailability and promotes vascular health[8]. Once dysfunctional, HDL may contribute to endothelial dysfunction[8]. Thus, assessing the properties of HDL is more informative than measuring its plasma levels alone[8].

Roux-en-Y gastric bypass surgery (RYGB) induces sustained weight loss in contrast to the limited success of pharmacological or behavioral interventions[9, 10]. Reduction in global and cardiovascular mortality [9, 11] and obesity-related co-morbidities[1, 10, 12, 13] have been reported after RYGB[1, 11]. The mechanisms underlying these beneficial effects are multiple[1, 11]. Amelioration of insulin resistance[14] or even resolution of T2DM occurs within days after RYGB, before any substantial weight loss. These findings suggested that glycemic control is restored by mechanisms[15, 16] related to the unique anatomical gut re-arrangement and the altered flow of nutrients after RYGB[10], rather than simply as the consequence of weight loss[15,

[17]. After RYGB, the modified entero-hepatic circulation of bile acids increases their intraluminal and systemic concentrations. Thus, elevated levels of these acids and undigested chyme may modify the release of gastrointestinal hormones[17]. In particular, plasma levels of the gut hormone glucagon-like peptide-1 (GLP-1) increase rapidly after RYGB, but not after dietary restriction, despite a similar weight loss[15, 16, 18]. These observations raised the hypothesis that changes in GLP-1 levels mediate the rapid and surgery-specific metabolic improvement achieved after RYGB[18, 19]. Drugs targeting the GLP-1 system are used in clinical practice as anti-diabetic agents with potential weight-lowering effects[20]. Beyond its metabolic actions, GLP-1 exhibits multiple beneficial properties, in particular anti-oxidant and endothelium-protective effects[19, 21].

Therefore, the present study was designed to evaluate whether RYGB causes a rapid improvement in endothelial function and restores the protective properties of HDL. Moreover, the experiments examined whether increased GLP-1 levels mediate the rapid metabolic and cardiovascular improvements associated with RYGB and if results of the procedure in obese rat can be translated to obese patients.

Materials and Methods

An expanded description of methods is available in supplemental online materials (SOM).

Animals and organ chamber experiments

Male Wistar rats were fed a high fat high cholesterol diet containing 60% kcal fat and 1.25% cholesterol for seven weeks prior and after surgery to achieve diet-induced obesity. Two main experiments were performed (SOM Fig. 1) with: a.) RYGB[22], sham-operated rats either fed *ad libitum* (controls) or weight-matched to RYGB and followed up for eight days. b.) Rats randomized to two treatment groups for the eight days of follow-up: controls treated with either vehicle or liraglutide (0.2 mg/kg twice daily) and RYGB treated with either vehicle or exendin$_{9\text{-}39}$ (10ug/kg/h). In addition, some rats were followed-up for one month after surgery. All animal experiments were approved by the Zurich Cantonal Veterinary Office. Cumulative concentration-relaxation curves in response to insulin and GLP-1 were obtained in rings of thoracic aorta as described[23].

Endothelium-protective properties of HDL

HDL was isolated from rat and patient serum by sequential density ultracentrifugation[6, 7]. HDL-stimulated NO production by cultured human aortic endothelial cells (HAEC) was tested *in vitro* using the fluorescent probe 4,5-diaminofluorescein (DAF-2)[7]. HDL anti-apoptotic properties were assessed in HAEC[24]. Arylesterase activity of HDL-associated paraoxonase-1 (PON-1) was measured by UV spectrophotometry[7]. Endothelial protein expression of vascular cell adhesion molecule 1 (VCAM-1) was determined in TNF-α stimulated (100pg/ml) HAEC treated with HDL[7]. NADPH oxidase activity was measured using a commercial assay kit.

Patient population

The surgery group consisted of 29 patients undergoing primary laparoscopic proximal RYGB[25]. The BMI-matched group consisted of 29 obese patients matched for BMI, body weight, age and gender to the RYGB group at week 12 after surgery. Moreover, 28 normal-weight volunteers matched for age and sex were enrolled. The Local Research and Ethics committee approved the study. All patients gave written consent

Statistical Analysis

Continuous variables with no/mild skew were presented as mean ± SEM; skewed measures as median and inter-quartile ranges (IQR). Discrete variables were summarized as frequencies and percentages. The distribution of the data was analyzed with one-sample Shapiro-Wilk test. Logarithmic transformation was performed to achieve normal distribution for skewed variables. Categorical variables were compared with χ^2 test or Fisher exact test, as appropriate. Continuous data were compared by use of the 2-tailed paired or unpaired *t* test (for normally distributed data sets) or the Mann-Whitney *U* or Wilcoxon signed-rank test (for skewed variables). We used a two-way ANOVA with repeated measures to compare repeated measurements on the same animals. For studying the complete outcome of each variable over time, we applied the linear mixed model using unstructured covariance matrix for quantitative variables. All tests were two-sided and statistical significance was accepted if the null hypothesis could be rejected at $p<0.05$. The authors had full access to and take full responsibility for the integrity of the data. All authors have read and agree to the manuscript as written.

Results

GLP-1 and bile acids plasma levels increase rapidly after RYGB

Fasting circulating GLP-1 levels were significantly higher in RYGB than in sham-operated rats (Fig. 1A-B and SOM Fig. 2A). RYGB receiving exendin$_{9\text{-}39}$ had GLP-1 levels similar to RYGB (Fig. 1B). Fasting plasma bile acid levels were increased after RYGB in all experiments (Fig 1C-D and SOM Fig. 2B) and were not affected significantly by either liraglutide or exendin$_{9\text{-}39}$.

The rapid improvement of vascular function after RYGB is weight-independent

Physiologically, insulin and GLP-1 induce NO-mediated endothelium-dependent relaxations[19, 26], whereas decreased NO bioavailability in obesity impairs endothelial function[2, 3, 26] . Therefore, the impact of RYGB on relaxations in response to increasing concentrations of both hormones was tested. Pre-incubation of the aortic rings with the NO synthase (NOS)-inhibitor Nω-nitro-L-arginine methyl ester (L-NAME) abolished endothelium-dependent relaxations in response to both hormones, indicating an NO-dependent mechanism (data not shown). The relaxing effect of GLP-1 was inhibited by incubation of the aortic rings with the specific GLP-1 receptor antagonist, exendin$_{9\text{-}39}$ (10^{-5} mol/L) (SOM Fig. 4A).

The responses to insulin and GLP-1, improved significantly eight days after RYGB, but not in weight-matched rats (Fig. 2A-B; SOM Fig.3 A-B). Acetylcholine-induced relaxations were also restored rapidly after RYGB (SOM Fig. 4B). One month after surgery, responses to both insulin and GLP-1 remained impaired in controls and weight-matched rats, but the

acetylcholine-induced relaxation improved similarly in aortae of weight-matched and RYGB rats (SOM Fig. 3 E-F and SOM Fig. 4 D-F).

RYGB improves endothelial function by a GLP-1 receptor-dependent mechanism

To investigate the role of GLP-1 in the improved relaxation after RYGB, the GLP-1 receptor antagonist, exendin$_{9\text{-}39}$ or the GLP-1 analog, liraglutide, were administered for eight days after RYGB (RYGB$_{\text{-exendin9-39}}$) or to control (controls$_{\text{-liraglutide}}$) rats, respectively. The relaxations improved in response to insulin and GLP-1 in controls$_{\text{-liraglutide}}$ compared to controls, thus mimicking RYGB's effects (Fig. 2 C-D). Instead, RYGB$_{\text{-exendin9-39}}$ rats had blunted relaxations to insulin and GLP-1 compared to RYGB, i.e. they were not significantly different from controls (Fig. 2 C-D and SOM Fig.3 C-D). Relaxations to acetylcholine in RYGB$_{\text{-exendin9-39}}$ were similar to those of RYGB rats (SOM Fig 4G). Relaxations to the endothelium-independent vasodilator sodium nitroprusside were similar among all experimental groups (SOM Fig. 4 C, H).

Vascular GLP-1 signaling is increased in RYGB rats independently of weight loss

Consistent with the improved relaxations to GLP-1 seen after RYGB, the aortic GLP-1 receptor expression was increased in RYGB compared to sham-operated rats eight days after surgery (Fig 3A).

Insulin and GLP-1-signaling in endothelial cells results in phosphorylation of protein kinase Akt at serine 473 (pSer^{473}-Akt) followed by phosphorylation of eNOS on Ser1177 (pSer^{1177}eNOS), a well-known eNOS-activating pathway [24, 27]. The phosphorylation level of pSer^{473}-Akt was significantly higher after RYGB compared to control rats (Fig 3B, Fig 4A)

and in controls$_{\text{-liraglutide}}$ compared to their controls, while it was reduced in RYGB$_{\text{-exendin9-39}}$ (Fig 4 A).

Obesity increases c-Jun amino terminal kinases (JNK) activity, which in turn impairs insulin and GLP-1 signaling[28, 29]. JNK phosphorylation (p-JNK) was reduced significantly after RYGB compared to sham-operated groups (Fig 3C). Exendin$_{9\text{-}39}$ prevented the reduction in JNK phosphorylation after RYGB. Controls$_{\text{-liraglutide}}$ rats had slightly decreased JNK activation compared to controls, but the degree of inhibition was lower than after RYGB (Fig. 4 B).

NO bioavailability was preserved after RYGB compared to sham-operated groups as reflected by an increased pSer^{1177}eNOS and decreased inhibitory Thr^{495} phosphorylation of eNOS[30], a higher eNOS dimer-to-monomer ratio and an augmented aortic NO production (Fig 3 D-G). Moreover, in RYGB we observed a lower eNOS-glutathionylation, which impairs the enzyme function[31], compared to weight-matched rats (SOM Fig.5A). Despite an only slightly higher pSer^{1177}eNOS, pThr^{495} was reduced, and dimerization of eNOS and NO production were increased in controls$_{\text{-liraglutide}}$ aortae to levels comparable to RYGB; by contrast, eNOS activation and NO production were reduced in RYGB$_{\text{-exendin9-39}}$. However, eNOS-glutathionylation was not affected by GLP-1 modulation (Fig 4 C-F, SOM Fig.5 B).

Decreased oxidative stress contributes to the preserved NO bioavailability after RYGB

High oxidative stress in obesity leads to NO inactivation by superoxide anions (O_2^-) and may impair endothelial NO availability. Concurrent with this notion, the addition of the free radical scavenger Polyethylene Glycol–Superoxide Dismutase (PEG-SOD) significantly improved relaxations in response to insulin and GLP-1 in both sham-operated rats. In RYGB and in controls$_{\text{-liraglutide}}$ PEG-SOD did not modify relaxations, suggesting that the level of oxidative stress was reduced by the surgery and liraglutide. Instead PEG-SOD was beneficial

in RYGB$_{\text{-exendin9-39}}$ confirming the important vascular antioxidant effect of GLP-1 and analogs (SOM Fig. 4 I-N). In addition, O_2^- concentration and NADPH oxidase activity, which is a major oxidant enzyme system producing O_2^- in the vasculature[6], were decreased in aortae of rats after RYGB compared to controls and weight-matched rats (Fig 5 A-C). In controls, treatment with liraglutide reduced aortic O_2^- concentration (Fig5A-B) and also, though to a lesser extent, aortic NADPH oxidase activity, mimicking RYGB; instead, exendin$_{9\text{-}39}$ treatment after RYGB did not counteract these antioxidant effects (Fig.5 C).

Endothelium-protective properties of HDL improve rapidly after RYGB

Endothelium-protective properties of HDL and the role of the increased circulating GLP-1 levels as mediators of the observed changes were assessed. In parallel to the rat studies, similar experiments were performed with HDL obtained from patients before, 14 days and 12 weeks after RYGB and from the BMI-matched group. See SOM Tables 1-2 for patient characteristics.

HDL-stimulated endothelial NO production increases rapidly after RYGB

HDL isolated from RYGB rats induced higher endothelial-NO production in HAEC than HDL from controls (Fig 6 A). Furthermore, HDL from controls$_{\text{-liraglutide}}$ rats stimulated endothelial NO production in a similar fashion as HDL isolated after RYGB. This effect was independent of GLP-1 receptor activation because it was preserved in RYGB rats treated with exendin$_{9\text{-}39}$ (Fig. 6 D).

The capacity of HDL isolated from patients to stimulate NO production increased already at day 14 and was normalized 12 weeks after RYGB compared to the pre-operative period (Fig 7A). The NO production stimulated by HDL isolated from the BMI-matched group was reduced compared to patients 12 weeks after RYGB. Accordingly, HAEC stimulated with HDL isolated from patients at day 14 and week 12 after RYGB exhibited improved eNOS

dimerization relative to their pre-operative HDL; eNOS dimerization was impaired in the BMI-matched group compared to 12W ($p< 0.055$) (Fig 7B).

HDL reduces endothelial cell apoptosis rapidly after RYGB

Compared to controls, HDL isolated after RYGB markedly reduced endothelial apoptosis induced by serum and growth factors deprivation (Fig. 6B). HDL from controls$_{\text{-liraglutide}}$ reduced endothelial apoptosis to a similar degree as after RYGB, but again treatment with exendin$_{9\text{-}39}$ after RYGB did not influence this property of HDL (Fig. 6E).

In patients, the capacity of HDL to inhibit endothelial apoptosis, which was impaired pre-operatively, was restored after surgery and resembled that of healthy subjects. The anti-apoptotic capacity of HDL was similar between patients 12 weeks after RYGB and their BMI-matched group (Fig. 7C).

Anti-Inflammatory properties of HDL improve after RYGB

HDL isolated after RYGB reduced TNFα–stimulated endothelial VCAM-1 expression significantly more than HDL from controls (Fig. 6C). HDL from controls$_{\text{-liraglutide}}$ rats was similarly effective as HDL isolated after RYGB, whereas treatment of RYGB rats with exendin$_{9\text{-}39}$ had no effect. Hence, the increase in anti-inflammatory properties of HDL following RYGB is mimicked by the GLP-1 analogue, but does not involve the activation of the known GLP-1 receptor (Fig. 6F). Endothelial VCAM-1 expression was reduced by HDL from patients 12 weeks after RYGB, but not by HDL from BMI-matched subjects (Fig 7D).

PON-1 activity increases rapidly after RYGB

PON-1 activity was increased after RYGB compared to controls. The improvement of PON-1 activity was surgery-specific, but independent of GLP-1 levels or signaling, because treatment with liraglutide or exendin$_{9\text{-}39}$ did not modify it compared to the respective control

groups (SOM Fig. 6 A, C). In patients, PON-1 activity improved progressively after RYGB, instead it was impaired in the BMI-matched group (Fig 7 E).

RYGB improves the capacity of HDL to stimulate macrophage cholesterol efflux

HDL after RYGB increased cholesterol efflux from J774 macrophages compared to HDL from sham-operated rats. Instead, HDL from controls$_{\text{-liraglutide}}$ or RYGB$_{\text{-exendin9-39}}$ did not change this parameter compared to HDL from the respective controls, suggesting that the RYGB-induced effect is independent of changes in GLP-1 levels or signaling (SOM Fig. 6B, D). In patients 12 weeks post-RYGB, HDL improved the cholesterol efflux capacity, in contrast to HDL from the BMI-matched group (Fig 7F).

RYGB rapidly restores the endothelial anti-oxidant effects of HDL

In HAEC, stimulation with HDL isolated after RYGB or controls$_{\text{-liraglutide}}$ reduced NADPH oxidase activity compared to HDL from sham-operated animals; exendin$_{9\text{-}39}$ treatment after RYGB did not alter HDL anti-oxidant effects (Fig5D). Endothelial NADPH oxidase activity was reduced by HDL from patients 12 weeks post-RYGB, but not by HDL from the BMI-matched group (Fig.5E).

Discussion

RYGB induces stable weight loss, improves obesity-associated co-morbidities and reduces cardiovascular mortality[1, 11]. Here we show that the beneficial metabolic and cardiovascular effects of RYGB likely result from changes in intestinal physiology rather than from weight loss alone. In particular, the gut hormone GLP-1, which increases rapidly after RYGB and restores glycemic homeostasis, may also contribute to the cardiovascular protection after surgery[19, 32]. Indeed, we found in the present study that: (1) in a rat model of RYGB, higher plasma levels of GLP-1 and bile acids were associated with increased aortic NO bioavailability, improved endothelium-dependent relaxation and normalized endothelium-protective properties of HDL; (2) GLP-1-dependent signaling was selectively activated in rat aortae after RYGB and was independent of weight loss; (3) treatment of control rats with the GLP-1 analog liraglutide for eight days improved both endothelial and HDL function, thus mimicking the effects of RYGB; and (4) in morbidly obese patients, increased plasma levels of GLP-1 and bile acids after RYGB were associated with a rapid improvement in endothelium-protective properties of HDL. The major results and proposed underlying mechanisms are summarized in Figure 8 and SOM Table 3.

Improved endothelium-dependent relaxations after RYGB involves a GLP-1-dependent mechanism

Beyond widespread metabolic actions, GLP-1 and its analogues affect the cardiovascular system[33] and in particular endothelial cells[19, 32], but also lipid metabolism[32, 34, 35]. GLP-1 exerts potent anti-oxidant effects[36], and possesses anti-apoptotic and anti-inflammatory properties in endothelial cells[24, 37]. The endothelial effects of GLP-1 are NO-mediated[38] and can be either dependent or independent of the activation of the known GLP-1 receptor[33].

Physiologically, GLP-1 promotes endothelial health indirectly by triggering insulin production[38] and by activating its own endothelial signaling pathways[32, 34, 35].

The present findings demonstrate that increased plasma levels of GLP-1 after RYGB, activate GLP-1 receptor-dependent intracellular signaling and induce a rapid restoration of endothelium-dependent relaxations. These beneficial effects were weight-independent, because they were absent in rats which had a weight loss matched to RYGB. One month after surgery, relaxations to insulin and GLP-1 remained impaired in weight-matched compared to RYGB rats; this points out that weight loss achieved by food restriction is not sufficient to induce all the beneficial effects of RYGB. Moreover, the persistent impairment of insulin and GLP-1-mediated endothelium-dependent relaxations suggest that the two hormones, which are partial agonists for the activation of endothelial NO release[3], are a more sensitive tool compared to acetylcholine to investigate how metabolic modifications influence endothelial function[3, 26].

The endothelial Akt/eNOS pathway mediates GLP-1 receptor-dependent vascular effects and represents also the major signaling cascade activated by insulin. This pathway was rapidly up-regulated in aortae after RYGB as well as after liraglutide treatment in controls, but was blunted by administration of the antagonist exendin$_{9\text{-}39}$ after RYGB.

Further, the phosphorylation of JNK was reduced after RYGB and less potently so in control$_{\text{-liraglutide}}$, but increased in RYGB$_{\text{-exendin9-39}}$. JNK is a crucial mediator of insulin resistance in obesity[29] and of endothelial dysfunction and oxidative stress[23]. Moreover, the inhibition of JNK signaling after administration of GLP-1 analogs protects endothelial cells against lipotoxicity-induced apoptosis and "eNOS uncoupling"[24].

Indeed, obesity-induced oxidative stress impairs NO bioavailability[3]; this was confirmed by the significant improvement of relaxations with the free radical scavenger PEG-SOD in sham operated rats, but not in RYGB or controls$_{\text{-liraglutide}}$. Accordingly, NADPH oxidase activity and O_2^- concentration decreased rapidly after RYGB or in controls$_{\text{-liraglutide}}$. As a consequence

of reduced aortic oxidative stress, "eNOS uncoupling"[3, 24] which causes dysfunction of the enzyme, was prevented in RYGB as shown by higher dimerization and lower glutathionylation of eNOS. This explains the improved NO-dependent relaxations in RYGB compared to weight-matched or exendin$_{9\text{-}39}$ treated RYGB rats. Like in RYGB, restored eNOS activity was paralleled by increased NO production after treatment with liraglutide. Hence, elevated GLP-1 levels and activation of GLP-1 receptor signaling play a key role in the improved endothelium-dependent vasodilatation after RYGB, independently of weight loss.

Rapid improvement of endothelium-protective properties of HDL after RYGB involve a GLP-1-dependent mechanism

Favorable lipid effects, i.e. higher HDL-C combined with lower LDL-C and TG levels, have been reported during long-term follow-up of patients after RYGB[4, 11]. The hormonal changes after RYGB are likely to influence lipid metabolism in addition to the weight loss *per se*, as suggested by the persistence of a beneficial lipid profile even in the fate of weight regain after surgery[39].

The present experiments demonstrate a specific effect of RYGB on HDL-mediated endothelial protection. HDL isolated after RYGB increased endothelial NO release, decreased endothelial apoptosis and expression of the adhesion molecule VCAM-1. Furthermore, the anti-oxidant activity of HDL and the capacity of the lipoprotein to stimulate cholesterol efflux from macrophages were also potentiated. All these protective effects did not improve in weight-matched rats, suggesting a weight-independent effect of RYGB. The most likely explanation for these weight–independent effects is the activation of the endothelial Akt/eNOS pathway after RYGB, which is the main pathway involved in the HDL-mediated NO release[7], and its anti-apoptotic[40], anti-oxidant[7] and anti-inflammatory properties[6, 8].

Likewise, HDL isolated from controls$_{\text{-liraglutide}}$ improved NO release, decreased endothelial apoptosis, oxidative stress and VCAM-1 expression similarly to that obtained from animals undergoing RYGB, suggesting a novel effect mediated by GLP-1. Hence, increased plasma levels of GLP-1 after RYGB exert protective endothelial effects via (1) improved HDL-cholesterol properties; (2) direct activation of endothelial signaling pathways; and (3) insulin-dependent vascular effects.

Despite the effect of RYGB on the properties of HDL, no difference was observed in total cholesterol concentrations in rats after RYGB. However, the cholesterol distribution profile was changed towards smaller size HDL-cholesterol particles compared to sham-operated groups in which cholesterol eluted in larger particles (SOM Fig. 7), as described in animals fed high cholesterol[41]. These changes in cholesterol distribution profile may be linked directly to the improved properties of HDL after RYGB.

GLP-1 analogs favorably modulate lipid metabolism in enterocytes and hepatocytes[42]. Here, liraglutide treatment resulted in smaller HDL-cholesterol particles, shifting the cholesterol distribution profile towards that seen after RYGB. Again, this effect does not seem to be mediated by the known GLP-1 receptor as shown by the lack of effect of exendin$_{9\text{-}39}$.

Translational relevance of the rapid improvement of endothelial protective properties of HDL after RYGB

RYGB rapidly improved the endothelial protective properties of HDL in severely obese patients and thus conferred a translational relevance to the experimental animal data. Indeed, HDL isolated 14 days after RYGB improved endothelial NO release as a consequence of restored eNOS dimerization. Preserved NO bioavailability was paralleled by reduced endothelial NADPH oxidase activity, apoptosis and VCAM-1 expression, but also a higher

PON-1 activity and HDL-stimulated cholesterol efflux capacity. In a previous study, HDL isolated from obese adolescents one-year after RYGB did not improve pSer^{1177}eNOS[43]. This result may be related to the fact that the assessment of eNOS activation was done by pSer^{1177}eNOS alone; whereas NO release measurement combined to eNOS-dimerization, as performed here, may be more informative to assess disturbances of NO bioavailability[3]. Results obtained in the present study appear to be applicable to both genders, while previous reports involved mainly women[5, 44]. Furthermore, the properties of HDL improved 12 weeks after RYGB to the level of healthy subjects, although the patients were still obese. Moreover, HDL properties were impaired in BMI-matched patients.

These observations suggest that the degree of weight and BMI loss induced by surgery is not sufficient or critical *per se* to improve the protective properties of HDL[5, 44]. Diet-induced weight loss is not associated with increased circulating GLP-1 and does not improve HDL properties [43, 45]. In future studies, it will be relevant to evaluate the impact on endothelial protective HDL properties of the other two most commonly performed bariatric surgery procedures: vertical sleeve gastrectomy and gastric banding[1]. Sleeve gastrectomy produces enhanced GLP-1 secretion and improvements in T2DM, independently from weight loss similar to RYGB. On the other hand, adjustable gastric banding, which is a restrictive procedure, is associated with comparably smaller increases in circulating GLP-1 or in other gut hormones[31].

Finally, RYGB normalized the fasting plasma levels of bile acids in patients, expanding a previous observation regarding the restoration of the post-prandial rise in bile acids after RYGB[46]. Circulating bile acids which were also elevated in the rats after RYGB, interact with the endothelium and induce NO production via Akt/eNOS activation[47]; they reduce endothelial VCAM -1 expression[47] and improve the ability of HDL to stimulate cholesterol efflux. Therefore bile acids may have contributed directly to the improved endothelial

protective effects observed in the present study. However, since liraglutide treatment, in the absence of elevated bile acids levels, mimicked the beneficial metabolic effects of RYGB, GLP-1 signaling may be the dominating factor under the present experimental conditions.

A major strength of the present study is its translational nature. It highlights with the animal experiments that the cardiovascular effects of RYGB likely derive from more than simple weight loss and that increased GLP-1 signaling may play a critical role for some surgery-specific beneficial effects. The rapid improvement in the vascular protective properties of HDL applies also to morbidly obese patients undergoing RYGB.

Conclusion

The present study shows that RYGB exerts endothelium-protective effects beyond surgery-induced weight loss. These effects are mediated, at least in part, by GLP-1 and GLP-1 receptor signaling. These findings may allow the identification of less-invasive treatment strategies targeting molecular cardiovascular and metabolic pathways affected by obesity.

Acknowledgments

We thank Markus Bachschmid, Melroy Miranda, Maja Franziska Müller, Silvija Radosavljevic and Nicole Kachappilly for technical help.

This work was supported in part by grants of the Swiss National Research Foundation (Nr. #310030-135815), the Fondation Leducq, Paris (Transatlantic Network on HDL Dysfunction), the University of Zurich (Forschungskredit and Center of Integrative Human Physiology), the Swiss Heart Foundation, the Hartmann Müller Foundation, the European Union (RESOLVE), and the Foundation for Cardiovascular Research–Zurich Heart House, Zurich, Switzerland.

There are no conflicts-of-interest, no author received honoraria or grants for the experiments described here.

Disclosures

None.

Figures legends

Figure 1.

Plasma levels of GLP-1 (A) and total bile acids (BA) (C) in RYGB compared to sham-operated rats after surgery and after GLP-1 modulation for eight days (B) and (D). The elevated GLP-1 concentrations measured in sham control$_{\text{-liraglutide}}$, probably reflected a cross-reactivity of the assay with liraglutide. (*p<0.0001 RYGB vs. sham-operated rats; § RYGB and RYGB$_{\text{-exendin9-39}}$ vs. controls and controls$_{\text{-liraglutide}}$; ° controls vs. controls$_{\text{-liraglutide}}$, p<0.002). Results are shown as mean ± SEM, n= 10-15 per group.

Figure 2.

A-B Relaxation of aortic rings isolated eight days after RYGB compared to sham-operated rats. Concentration–response curves during submaximal contraction to norepinephrine (NE) in response to insulin (A) and GLP-1 (B) (* sham-operated rats vs. RYGB; § controls vs. weight-matched, ° RYGB vs weight-matched, $p < 0.05$).

C-D Effect of GLP-1 modulation for eight days on the relaxations to insulin (C) or GLP-1 (D) (# RYGB vs. controls; ~ RYGB vs. RYGB$_{\text{-exendin9-39}}$; ° control$_{\text{-liraglutide}}$ vs. controls; *controls$_{\text{-liraglutide}}$ and RYGB vs. other study groups, $p < 0.05$), n= 6- 8 per group.

Figure 3.

GLP-1 receptor (GLP-1R) (A), pSer^{473}-Akt (B) and p-JNK (C) protein expression from aortae isolated eight days after RYGB compared to sham-operated rats. eNOS protein Ser^{1177} (D) and Thr^{495} (E) phosphorylation and eNOS dimerization (F). Representative Western blots and densitometric quantification are shown. (G) Electron spin resonance spectroscopy analysis of

aortic NO production (* RYGB vs. other groups; § weight-matched vs. controls, $p< 0.05$), n=6-8 per group.

Figure 4.

(A) $pSer^{473}$-Akt and p-JNK (B) protein expression from aortae isolated eight days after GLP-1 modulation. eNOS protein Ser^{1177} (C), Thr^{495} (D) phosphorylation and eNOS dimerization (E). (F) Electron spin resonance spectroscopy analysis of aortic NO production (* RYGB vs. other groups; # $controls_{\text{-liraglutide}}$ vs. controls, § $controls_{\text{-liraglutide}}$ vs. $RYGB_{\text{-exendin9-39}}$, $p< 0.05$), n=6-8 per group.

Figure 5.

Fluorescence detection of superoxide anions in rat aortae labeled with red-dihydroethidium (DHE) staining (A) and relative quantification (B). Nicotinamide adenine dinucleotide phosphate (NADPH) oxidase activity was measured in rat aortae (C) and in HAEC after stimulation with HDL(D) isolated from rats after RYGB and after GLP-1 modulation (* RYGB vs. controls; §$RYGB_{\text{-exendin9-39}}$ vs. sham-operated rats, $p\leq 0.05$; # $control_{\text{-liraglutide}}$ vs. sham-operated rats, $p< 0.05$). (E) NADPH oxidase activity in HAEC stimulated with HDL isolated preoperatively (D0), at day 14 (D14), at 12 weeks (W12) post-RYGB and in BMI-matched patients (*D0 vs W12; ç W12 vs BMI-matched, $p< 0.05$), n= 13 RYGB patients, 10 healthy subjects and 9 BMI-matched patients.

Figure 6.

Endothelial NO production after HAEC stimulation with HDL isolated post RYGB (A) and after GLP-1 modulation (D). Endothelial anti-apoptotic effects (B) and endothelial anti-inflammatory effect (C) of HDL after RYGB and after GLP-1 modulation (E, F, respectively)

(*RYGB vs. other groups; § controls vs. weight-matched; # controls vs. control$_{-liraglutide}$;° controls vs. RYGB$_{-exendin9-39}$, p<0.05), n=8-10 per group. SW indicates serum withdrawal.

Figure 7.

Endothelial NO production after HAEC stimulation with HDL isolated preoperatively (D0), at day 14 (D14) and 12 weeks (W12) post-RYGB, in BMI-matched patients and in healthy subjects, (n= 29 RYGB patients, 28 healthy subjects, 29 BMI-matched) (A). HDL-mediated eNOS activation measured by eNOS dimerization (n= 10 RYGB, 5 healthy, 6 BMI-matched) (B); endothelial anti-apoptotic effect (n= 29 RYGB, 28 healthy, 28 BMI-matched) (C); and anti-inflammatory effect of HDL on TNF-α–stimulated HAEC (n= 29 RYGB, 27 healthy, 29 BMI-matched) (D). HDL associated PON-1 activity (n= 29 RYGB, 28 healthy, 28 BMI-matched) (E) and HDL-stimulated macrophage cholesterol efflux (n= 28 RYGB, 28 healthy, 29 BMI-matched) (F) (°D0 vs healthy; §D0 vs D14; *D0 vs W12; ΦD14 vs W12, #W12 vs healthy, ç W12 vs BMI-matched, p< 0.05). SW indicates serum withdrawal.

Figure 8.

Proposed cellular mechanisms involved in the beneficial effects of RYGB on endothelial function and HDL vaso-protective properties. The bioavailability of NO is decreased in obesity. Rapidly after RYGB, elevated GLP-1 levels through the activation of the GLP-1 receptor activates the pSer^{473}-Akt cascade enhancing peNOSer^{1177}and eNOS dimerization while reducing peNOSThr^{495}, JNK phosphorylation, NADPH oxidase activity and anion superoxide (O_2^-) production. This leads to higher NO levels and thus improved endothelial function. These effects are mimicked by liraglutide treatment of control rats and are blocked by exendin$_{9-39}$ after RYGB. RYGB surgery and liraglutide improved also HDL-mediated NO production, endothelial anti-apoptotic, anti-oxidant and anti-inflammatory properties. The latter properties are independent of the activation of the known GLP-1 receptor and not

blocked by exendin$_{9\text{-}39}$. HDL-associated PON-1 activity and cholesterol efflux improve after RYGB independently of GLP-1 modulation.

References

1. Poirier P, Cornier MA, Mazzone T, Stiles S, Cummings S, Klein S, McCullough PA, Ren Fielding C, Franklin BA, American Heart Association Obesity Committee of the Council on Nutrition PA, Metabolism. Bariatric surgery and cardiovascular risk factors: A scientific statement from the american heart association. *Circulation*. 2011;123:1683-1701
2. Sansbury BE, Cummins TD, Tang Y, Hellmann J, Holden CR, Harbeson MA, Chen Y, Patel RP, Spite M, Bhatnagar A, Hill BG. Overexpression of endothelial nitric oxide synthase prevents diet-induced obesity and regulates adipocyte phenotype. *Circ Res*. 2012;111:1176-1189
3. Mauricio MD, Aldasoro M, Ortega J, Vila JM. Endothelial dysfunction in morbid obesity. *Curr Pharm Des*. 2013;19:5718-5729
4. Bays HE, Toth PP, Kris-Etherton PM, Abate N, Aronne LJ, Brown WV, Gonzalez-Campoy JM, Jones SR, Kumar R, La Forge R, Samuel VT. Obesity, adiposity, and dyslipidemia: A consensus statement from the national lipid association. *J Clin Lipidol*. 2013;7:304-383
5. Asztalos BF, Swarbrick MM, Schaefer EJ, Dallal GE, Horvath KV, Ai M, Stanhope KL, Austrheim-Smith I, Wolfe BM, Ali M, Havel PJ. Effects of weight loss, induced by gastric bypass surgery, on hdl remodeling in obese women. *J Lipid Res*. 2010;51:2405-2412
6. Sorrentino SA, Besler C, Rohrer L, Meyer M, Heinrich K, Bahlmann FH, Mueller M, Horvath T, Doerries C, Heinemann M, Flemmer S, Markowski A, Manes C, Bahr MJ, Haller H, von Eckardstein A, Drexler H, Landmesser U. Endothelial-vasoprotective effects of high-density lipoprotein are impaired in patients with type 2 diabetes mellitus but are improved after extended-release niacin therapy. *Circulation*. 2010;121:110-122
7. Besler C, Heinrich K, Rohrer L, Doerries C, Riwanto M, Shih DM, Chroni A, Yonekawa K, Stein S, Schaefer N, Mueller M, Akhmedov A, Daniil G, Manes C, Templin C, Wyss C, Maier W, Tanner FC, Matter CM, Corti R, Furlong C, Lusis AJ, von Eckardstein A, Fogelman AM, Luscher TF, Landmesser U. Mechanisms underlying adverse effects of hdl on enos-activating pathways in patients with coronary artery disease. *J Clin Invest*. 2011;121:2693-2708
8. Luscher TF, Landmesser U, von Eckardstein A, Fogelman AM. High-density lipoprotein: Vascular protective effects, dysfunction, and potential as therapeutic target. *Circ Res*. 2014;114:171-182
9. Raffaelli M, Guidone C, Callari C, Iaconelli A, Bellantone R, Mingrone G. Effect of gastric bypass versus diet on cardiovascular risk factors. *Ann Surg*. 2014;259:694-699
10. Ikramuddin S, Korner J, Lee WJ, Connett JE, Inabnet WB, Billington CJ, Thomas AJ, Leslie DB, Chong K, Jeffery RW, Ahmed L, Vella A, Chuang LM, Bessler M, Sarr MG, Swain JM, Laqua P, Jensen MD, Bantle JP. Roux-en-y gastric bypass vs intensive medical management for the control of type 2 diabetes, hypertension, and hyperlipidemia: The diabetes surgery study randomized clinical trial. *JAMA*. 2013;309:2240-2249
11. Adams TD, Davidson LE, Litwin SE, Kolotkin RL, LaMonte MJ, Pendleton RC, Strong MB, Vinik R, Wanner NA, Hopkins PN, Gress RE, Walker JM, Cloward TV, Nuttall RT, Hammoud A, Greenwood JL, Crosby RD, McKinlay R, Simper SC, Smith SC, Hunt SC. Health benefits of gastric bypass surgery after 6 years. *JAMA*. 2012;308:1122-1131

12. Mingrone G, Panunzi S, De Gaetano A, Guidone C, Iaconelli A, Leccesi L, Nanni G, Pomp A, Castagneto M, Ghirlanda G, Rubino F. Bariatric surgery versus conventional medical therapy for type 2 diabetes. *N Engl J Med*. 2012;366:1577-1585
13. Brethauer SA, Heneghan HM, Eldar S, Gatmaitan P, Huang H, Kashyap S, Gornik HL, Kirwan JP, Schauer PR. Early effects of gastric bypass on endothelial function, inflammation, and cardiovascular risk in obese patients. *Surg Endosc*. 2011;25:2650-2659
14. Faria G, Preto J, da Costa EL, Guimaraes JT, Calhau C, Taveira-Gomes A. Acute improvement in insulin resistance after laparoscopic roux-en-y gastric bypass: Is 3 days enough to correct insulin metabolism? *Obes Surg*. 2013;23:103-110
15. Laferrere B, Reilly D, Arias S, Swerdlow N, Gorroochurn P, Bawa B, Bose M, Teixeira J, Stevens RD, Wenner BR, Bain JR, Muehlbauer MJ, Haqq A, Lien L, Shah SH, Svetkey LP, Newgard CB. Differential metabolic impact of gastric bypass surgery versus dietary intervention in obese diabetic subjects despite identical weight loss. *Sci Transl Med*. 2011;3:80re82
16. Plum L, Ahmed L, Febres G, Bessler M, Inabnet W, Kunreuther E, McMahon DJ, Korner J. Comparison of glucostatic parameters after hypocaloric diet or bariatric surgery and equivalent weight loss. *Obesity (Silver Spring)*. 2011;19:2149-2157
17. Quercia I, Dutia R, Kotler DP, Belsley S, Laferrere B. Gastrointestinal changes after bariatric surgery. *Diabetes Metab*. 2014;40:87-94
18. Laferrere B, Teixeira J, McGinty J, Tran H, Egger JR, Colarusso A, Kovack B, Bawa B, Koshy N, Lee H, Yapp K, Olivan B. Effect of weight loss by gastric bypass surgery versus hypocaloric diet on glucose and incretin levels in patients with type 2 diabetes. *J Clin Endocrinol Metab*. 2008;93:2479-2485
19. Campbell JE, Drucker DJ. Pharmacology, physiology, and mechanisms of incretin hormone action. *Cell Metab*. 2013;17:819-837
20. Wadden TA, Hollander P, Klein S, Niswender K, Woo V, Hale PM, Aronne L. Weight maintenance and additional weight loss with liraglutide after low-calorie-diet-induced weight loss: The scale maintenance randomized study. *Int J Obes (Lond)*. 2013;37:1443-1451
21. Anagnostis P, Athyros VG, Adamidou F, Panagiotou A, Kita M, Karagiannis A, Mikhailidis DP. Glucagon-like peptide-1-based therapies and cardiovascular disease: Looking beyond glycaemic control. *Diabetes Obes Metab*. 2011;13:302-312
22. Bueter M, Abegg K, Seyfried F, Lutz TA, le Roux CW. Roux-en-y gastric bypass operation in rats. *J Vis Exp*. 2012:e3940
23. Osto E, Matter CM, Kouroedov A, Malinski T, Bachschmid M, Camici GG, Kilic U, Stallmach T, Boren J, Iliceto S, Luscher TF, Cosentino F. C-jun n-terminal kinase 2 deficiency protects against hypercholesterolemia-induced endothelial dysfunction and oxidative stress. *Circulation*. 2008;118:2073-2080
24. Erdogdu O, Eriksson L, Xu H, Sjoholm A, Zhang Q, Nystrom T. Exendin-4 protects endothelial cells from lipoapoptosis by pka, pi3k, enos, p38 mapk, and jnk pathways. *J Mol Endocrinol*. 2013;50:229-241
25. Weber M, Muller MK, Bucher T, Wildi S, Dindo D, Horber F, Hauser R, Clavien PA. Laparoscopic gastric bypass is superior to laparoscopic gastric banding for treatment of morbid obesity. *Ann Surg*. 2004;240:975-982; discussion 982-973
26. Baron AD. Insulin resistance and vascular function. *Journal of diabetes and its complications*. 2002;16:92-102
27. Rask-Madsen C, Li Q, Freund B, Feather D, Abramov R, Wu IH, Chen K, Yamamoto-Hiraoka J, Goldenbogen J, Sotiropoulos KB, Clermont A, Geraldes P, Dall'Osso C, Wagers AJ, Huang PL, Rekhter M, Scalia R, Kahn CR, King GL. Loss of insulin

signaling in vascular endothelial cells accelerates atherosclerosis in apolipoprotein e null mice. *Cell Metab*. 2010;11:379-389
28. Zhang L, Yang M, Ren H, Hu H, Boden G, Li L, Yang G. Glp-1 analogue prevents nafld in apoe ko mice with diet and acrp30 knockdown by inhibiting c-jnk. *Liver Int*. 2013;33:794-804
29. Hirosumi J, Tuncman G, Chang L, Gorgun CZ, Uysal KT, Maeda K, Karin M, Hotamisligil GS. A central role for jnk in obesity and insulin resistance. *Nature*. 2002;420:333-336
30. Fleming I, Fisslthaler B, Dimmeler S, Kemp BE, Busse R. Phosphorylation of thr(495) regulates ca(2+)/calmodulin-dependent endothelial nitric oxide synthase activity. *Circ Res*. 2001;88:E68-75
31. Galougahi KK, Liu CC, Gentile C, Kok C, Nunez A, Garcia A, Fry NA, Davies MJ, Hawkins CL, Rasmussen HH, Figtree GA. Glutathionylation mediates angiotensin ii-induced enos uncoupling, amplifying nadph oxidase-dependent endothelial dysfunction. *J Am Heart Assoc*. 2014;3:e000731
32. Sivertsen J, Rosenmeier J, Holst JJ, Vilsboll T. The effect of glucagon-like peptide 1 on cardiovascular risk. *Nat Rev Cardiol*. 2012;9:209-222
33. Ban K, Noyan-Ashraf MH, Hoefer J, Bolz SS, Drucker DJ, Husain M. Cardioprotective and vasodilatory actions of glucagon-like peptide 1 receptor are mediated through both glucagon-like peptide 1 receptor-dependent and -independent pathways. *Circulation*. 2008;117:2340-2350
34. Green BD, Hand KV, Dougan JE, McDonnell BM, Cassidy RS, Grieve DJ. Glp-1 and related peptides cause concentration-dependent relaxation of rat aorta through a pathway involving katp and camp. *Arch Biochem Biophys*. 2008;478:136-142
35. Nystrom T, Gonon AT, Sjoholm A, Pernow J. Glucagon-like peptide-1 relaxes rat conduit arteries via an endothelium-independent mechanism. *Regul Pept*. 2005;125:173-177
36. Laviola L, Leonardini A, Melchiorre M, Orlando MR, Peschechera A, Bortone A, Paparella D, Natalicchio A, Perrini S, Giorgino F. Glucagon-like peptide-1 counteracts oxidative stress-dependent apoptosis of human cardiac progenitor cells by inhibiting the activation of the c-jun n-terminal protein kinase signaling pathway. *Endocrinology*. 2012;153:5770-5781
37. Noyan-Ashraf MH, Shikatani EA, Schuiki I, Mukovozov I, Wu J, Li RK, Volchuk A, Robinson LA, Billia F, Drucker DJ, Husain M. A glucagon-like peptide-1 analog reverses the molecular pathology and cardiac dysfunction of a mouse model of obesity. *Circulation*. 2013;127:74-85
38. Nystrom T, Gutniak MK, Zhang Q, Zhang F, Holst JJ, Ahren B, Sjoholm A. Effects of glucagon-like peptide-1 on endothelial function in type 2 diabetes patients with stable coronary artery disease. *Am J Physiol Endocrinol Metab*. 2004;287:E1209-1215
39. Brolin RE, Bradley LJ, Wilson AC, Cody RP. Lipid risk profile and weight stability after gastric restrictive operations for morbid obesity. *J Gastrointest Surg*. 2000;4:464-469
40. Riwanto M, Rohrer L, Roschitzki B, Besler C, Mocharla P, Mueller M, Perisa D, Heinrich K, Altwegg L, von Eckardstein A, Luscher TF, Landmesser U. Altered activation of endothelial anti- and proapoptotic pathways by high-density lipoprotein from patients with coronary artery disease: Role of high-density lipoprotein-proteome remodeling. *Circulation*. 2013;127:891-904
41. Mahley RW, Weisgraber KH, Innerarity T, Brewer HB, Jr., Assmann G. Swine lipoproteins and atherosclerosis. Changes in the plasma lipoproteins and apoproteins induced by cholesterol feeding. *Biochemistry*. 1975;14:2817-2823

42. Xiao C, Dash S, Lewis GF. Mechanisms of incretin effects on plasma lipids and implications for the cardiovascular system. *Cardiovasc Hematol Agents Med Chem*. 2012;10:289-294
43. Matsuo Y, Oberbach A, Till H, Inge TH, Wabitsch M, Moss A, Jehmlich N, Volker U, Muller U, Siegfried W, Kanesawa N, Kurabayashi M, Schuler G, Linke A, Adams V. Impaired hdl function in obese adolescents: Impact of lifestyle intervention and bariatric surgery. *Obesity (Silver Spring)*. 2013;21:E687-695
44. Aron-Wisnewsky J, Julia Z, Poitou C, Bouillot JL, Basdevant A, Chapman MJ, Clement K, Guerin M. Effect of bariatric surgery-induced weight loss on sr-bi-, abcg1-, and abca1-mediated cellular cholesterol efflux in obese women. *J Clin Endocrinol Metab*. 2011;96:1151-1159
45. Aicher BO, Haser EK, Freeman LA, Carnie AV, Stonik JA, Wang X, Remaley AT, Kato GJ, Cannon RO, 3rd. Diet-induced weight loss in overweight or obese women and changes in high-density lipoprotein levels and function. *Obesity (Silver Spring)*. 2012;20:2057-2062
46. Ahmad NN, Pfalzer A, Kaplan LM. Roux-en-y gastric bypass normalizes the blunted postprandial bile acid excursion associated with obesity. *Int J Obes (Lond)*. 2013;37:1553-1559
47. Kida T, Tsubosaka Y, Hori M, Ozaki H, Murata T. Bile acid receptor tgr5 agonism induces no production and reduces monocyte adhesion in vascular endothelial cells. *Arterioscler Thromb Vasc Biol*. 2013;33:1663-1669

Rapid and body weight-independent improvement of endothelial function and HDL properties after Roux-en-Y gastric bypass: role of glucagon-like peptide-1.

SUPPLEMENTAL MATERIAL

°Elena Osto, MD,PhD[1, *]; Petia Doytcheva, Msc[1,2*];Caroline Corteville, MD[2]; Marco Bueter, MD,PhD[3], Claudia Dörig, Msc[2], Simona Stivala, PhD[1], Helena Buhmann, MD[2], Sophie Colin, PhD[4], Lucia Rohrer, PhD[5]; Reda Hasballa Msc[5], Anne Tailleux, PhD[4], Christian Wolfrum PhD[6], .Francesco Tona, MD,PhD[7], Jasmin Manz Msc[1], Diana Vetter, MD[3], Kerstin Spliethoff DVM[2], Paul M. Vanhoutte MD, PhD[8], Ulf Landmesser, MD[1], Francois Pattou, MD,PhD[9], Bart Staels MD[4], Christian M. Matter, MD[1], Thomas A. Lutz DVM,PhD[2*], and Thomas F. Lüscher MD[1*].

1 Centre for Molecular Cardiology, University of Zurich and University Heart Center, Cardiology, University Hospital Zurich, Switzerland, 2Institute of Veterinary Physiology, University of Zurich, Switzerland, 3Department of Surgery, University Hospital Zurich, Switzerland, 4 Université Lille 2, INSERM UMR1011, EGID, Institut Pasteur de Lille, Lille, France , 5Institute of Clinical Chemistry, University Hospital Zurich, Switzerland,6 Department of Health Sciences and Technology, ETH Zurich, Switzerland, 7Department of Cardiac, Thoracic and Vascular Sciences, University of Padua, Italy ,8State Key Laboratory for Pharmaceutical Biotechnologies &Department of Pharmacology & Pharmacy, LKS Faculty of Medicine, The University of Hong Kong, 9Department of Endocrine Surgery, Lille University Hospital, France.

Running title: rapid effects of RYGB on endothelial and HDL function

Address for Correspondence °Elena Osto, M.D., Ph.D.

Centre for Molecular Cardiology

University of Zurich

Wagistrasse, 12

CH-8952 Schlieren, Switzerland

Tel: 41-44-635 6469

Fax: 41-44-635 6827

Email: elena.osto@uzh.ch

*These authors contributed equally.

Supplementary Materials and Methods

Animals and housing

Adult male Wistar rats obtained from Janvier, France, weighted 250-300g at arrival. We performed a pilot experiment in order to define 1) the appropriate diet (high fat high cholesterol (HFHC) versus high fat (HF) only) to achieve diet-induced obesity (DIO) and impaired endothelial dysfunction; 2) the earliest time point for tissue harvesting and HDL isolation after RYGB in order to avoid the acute phase reaction post-surgical trauma and 3) the approximate amount of food eaten by the RYGB rats for weight matching of sham-operated rats in the subsequent tests (see below). Seven weeks of HFHC diet induced endothelial dysfunction in contrast to HF diet alone (data not shown). The acute phase reaction after RYGB was resolved on post-operative day 8 (D8) as indicated by the time courses of Interleukin (IL)-1β, tumor necrosis factor (TNF)-α and IL-6 (data not shown). For all subsequent experiments, rats were transferred to a commercial HFHC containing 60% kcal fat and 1.25% cholesterol (Research Diets, New Brunswick NJ, USA) for a period of 7 weeks prior to surgery; the same diet was offered post-surgery. Rats were initially housed 4 per cage in Makrolon cages (Indulab, Gams, Switzerland). One week before surgery, they were single housed in wire mesh cages until the end of the experimental period. Rats were housed in a colony room with an average temperature of 23°C and a 12-hour light/dark cycle. The groups of animals used for the following two main experiments were: 1.) RYGB or sham-surgery fed ad libitum (controls) or weight- matched to RYGB and followed for a D8 period (SOM Fig.1A); 2.) RYGB or controls followed for a D8 period and simultaneous *in vivo* GLP-1 intervention (SOM Fig.1B). Some parameters were also assessed in RYGB and sham-operated rats that were followed up for one month after surgery. The Cantonal Zurich Veterinary Office approved all animal experiments.

Surgeries

Rats were randomly allocated to either RYGB or sham-operations. For the first experiment, 24 rats with an average body weight of 590g underwent RYGB surgery, and 24 underwent sham-surgery, of which 12 with an average body weight of 592g were controls, and 12 with average body weight of 593g were weight-matched to RYGB.

For the second experiment with simultaneous GLP-1 intervention, 22 rats with an average body weight of 502g underwent RYGB surgery and 12 rats with an average body weight of 500g underwent sham-surgery.

For the third experiment, 24 rats with an average body weight of 526g underwent RYGB surgery, and 24 rats underwent sham-surgery, of which 12 with an average body weight of 531g were controls and 12 with an average body weight of 532g were weight-matched.

Anesthesia was induced in a chamber filled with 5% isoflurane in room air (1 L/min). After an adequate depth of anesthesia was achieved, rats were shaved from sternum to pelvis followed by disinfection with Betadine scrub (Mundi Pharma, Basel, Switzerland). Rats were then placed in a supine position on a heating pad and positioned in a nose cone to maintain anesthesia (2%–3% isoflurane in room air, 0.8 L/min) for the duration of the surgery. All surgeries were conducted as previously described[1]. Briefly, a midline incision of approximately 4 cm starting just below the xiphoid process was performed. For the RYGB procedure, the proximal small bowel was transected approximately 20 cm distal to the pylorus of the stomach, creating a proximal and distal end of small bowel. The proximal end, being still continuous with the remaining portion of the stomach, constituted the biliopancreatic limb and was anastomosed to the distal small intestine, approximately 25–30 cm from the cecum, creating the common channel. For formation of the gastric pouch, the stomach was transected approximately 5 mm below the gastro-esophageal junction, creating a pouch of a size of less than 5% of original stomach size. The Roux-en-Y reconstruction was completed by connecting the distal end of the proximal small bowel to the gastric pouch, leading to

formation of the alimentary (Roux) limb. One single RYGB procedure lasted approximately 100 minutes. For sham operations, an anterior gastrostomy with subsequent closure was performed. One single sham procedure lasted approximately 30 minutes. The abdominal wall and the skin were closed in layers after both operations.

No RYGB rats died during surgery. Immediately following surgery, each rat received 5 mL of saline subcutaneously to compensate for fluid loss. Rats were then placed under indirect red light in a polycarbonate cage until they fully recovered from anesthesia, at which time they were returned to their home cages. Baytril 10mg/kg (Bayer, Germany) and Carprofen 5mg/kg (Norocarp, Norbrook Laboratories) were administered before surgery and for two days post-surgery. Post-operatively, rats were fed HFHC diet and body weight and food intake were measured daily. Sham rats were randomly divided into controls or weight-matched rats; the latter were food-restricted (approximately 9-10 g/day based on the pilot experiment). Hence, the weight-matched group had a controlled food intake in order to match their weight to RYGB rats, this allowed the distinction between RYGB-specific from weight-dependent effects, since the only difference between these two study groups was RYGB surgery. During three-days post-operatively the HFHC solid diet was mixed with water to facilitate swallowing.

In vivo GLP-1 interventions

For the second experiment, sham-operated and RYGB rats were randomized to one of the following treatment groups, respectively: controls were treated with phosphate-buffered saline (PBS) (vehicle, n=6) or with liraglutide (controls-$_{\text{liraglutide}}$; 0.2 mg/kg twice daily), n=6; RYGB were treated with vehicle (n=11) or RYGB exendin$_{9\text{-}39}$ (10ug/kg/h), n=11. Liraglutide (Victoza; Novo Nordisk, Bagsvaerd, Denmark) or PBS vehicle were administered twice daily via subcutaneous (s.c.) injections for the eight-days follow-up period starting immediately post-surgery, with one injection in the light phase and one in the dark phase. The liraglutide

dose was increased stepwise over the first two treatment days (0.05 mg/kg, 0.1 mg/kg, 0.15 mg/kg, 0.2 mg/kg) and then maintained at 0.2 mg/kg per injection. Exendin$_{9\text{-}39}$ (Bachem, Bubendorf, Switzerland) or its vehicle was administered s.c. via osmotic minipumps (Alzet model 2001, Charles River, Germany) for the eight-days follow-up period. Implantation of the osmotic minipumps was performed immediately following the RYGB surgery while rats were still under anesthesia; minipumps were inserted via an incision made in the midscapular region. Dosages of liraglutide and exendin$_{9\text{-}39}$ were selected based on previous *in vivo* results[2-4].

Rat blood collection

Preoperative plasma was collected on the day of surgery in Microvette EDTA vacutainers (Sarstedt, Nümbrecht, Germany) supplemented with protease inhibitor cocktail (Sigma-Aldrich, Saint Louis, Missouri,USA) and DPPIV inhibitor (Millipore, Darmstadt, Germany) and was kept on ice until centrifugation. Serum was collected in Microvette vacutainers (Sarstedt) and kept at room temperature until centrifugation. After centrifugation the supernatant was separated and stored at -80°C. Postoperative blood was collected at the time of euthanasia by heart puncture.

Tissue harvesting

Human insulin (10 mU/g; Humalog, Lilly, Indianapolis, Indiana, USA) or saline vehicle were injected intra-peritoneally for studying insulin signaling and action in subsequent *ex vivo* experiments as described[5]. Ten minutes after injection, rats were sacrificed and organs were harvested within 30 minutes; rats were anesthetized by isoflurane inhalation. The entire aorta from the heart to the iliac bifurcation was excised and placed immediately in cold modified Krebs-Ringer bicarbonate solution (pH 7.4, 37°C, 95% O2, 5% CO2) of the following composition (mmol/L): NaCl (118.6), KCl (4.7), CaCl2 (2.5), KH2PO4 (1.2), MgSO4 (1.2),

NaHCO3 (25.1), glucose (11.1), and calcium EDTA (0.026). The aorta was cleaned from adhering connective tissue under a dissection microscope and either snap-frozen in liquid nitrogen and stored at -80°C or used immediately for *ex vivo* organ chamber experiments.

Organ chamber experiments

For endothelial function experiments[6], 2-3 mm long aortic rings were connected to an isometric force transducer (Multi-Myograph 610M, Danish Myo Technology A/S, Aarhus, Denmark), suspended in an organ chamber filled with 5 mL Krebs-Ringer bicarbonate solution (37°C, pH 7.4), and bubbled with 95% O2, 5% CO2 at 37°C. Isometric tension was recorded continuously. After a 30-minutes equilibration period, rings were gradually stretched to the optimal point of their length-tension curve as determined by the contraction in response to potassium chloride (100 mmol/L). Concentration-response curves were obtained in a cumulative fashion. Responses to acetylcholine (10^{-9} to 10^{-6} mol/L; Sigma-Aldrich), GLP-$1_{(7–36)}$ amide (10^{-12}-10^{-6}mol/L; herein referred to as GLP-1; Bachem) and insulin (10^{-11} to 10^{-6} mol/L; Humalog, Lilly) were recorded during submaximal contraction to norepinephrine (10^{-6} mol/L, Sigma-Aldrich, USA) in the presence or absence of Nω-nitro-L-arginine methyl ester (L-NAME, 10^{-4} mol/L, Sigma-Aldrich), a non-selective nitric oxide (NO) synthase inhibitor or of the free radical scavenger polyethylene glycol–superoxide dismutase (SOD 150 U/mL, Sigma-Aldrich). The NO donor sodium nitroprusside (SNP, 10^{-10} to 10^{-5} mol/L; Sigma-Aldrich) was added to test endothelium-independent relaxation. Relaxations were expressed as a percentage of the pre-contraction. In order to study the direct effects of GLP-1 on vascular function, cumulative concentration-relaxation responses were obtained for the peptide GLP-$1_{(7-36)}$ amide (10^{-12} to 10^{-6} mol/L, Bachem) in the presence or absence of the highly specific GLP-1 receptor antagonist exendin$_{9-39}$ (10^{-5}mol/L 10 min before adding GLP-1) (Bachem), L-NAME or PEG-SOD.

Western blotting

Frozen aortae were pulverized and dissolved in lysis buffer (120 mmol/L sodium chloride, 50 mmol/L Tris, 20 mmol/L sodium fluoride, 1 mmol/L benzamidine, 1 mmol/L dithiothreitol, 1 mmol/L EDTA, 6 mmol/L EGTA, 15 mmol/L sodium pyrophosphate, 0.8 ug/mL leupeptin, 30 mmol/L *p*-nitrophenyl phosphate, 0.1 mmol/L phenylmethylsulfonyl fluoride, and 1% NP-40) for immunoblotting. The samples (30 ug) were subjected to SDS-PAGE gel for electrophoresis and incubated with SAPK/JNK and phospho-SAPK/JNK (Thr183/Tyr185) antibodies (Cell Signalling, Beverly, Massachusetts, USA), anti-eNOS/NOS Type III and anti-eNOS (pS1177) antibodies (BD Biosciences, San Jose, CA, USA), anti-eNOS (pT495) (BD Biosciences), Akt and phospho-Akt (Ser473) antibodies (Cell Signalling), anti-GLP-1-R antibody (Abcam, Cambridge, UK) and anti-GAPDH antibody (Millipore). The immunoreactive bands were detected by chemiluminescence (Amersham Biosciences, Buckinghamshire, UK) and quantified densitometrically with Image J software (National Institutes of Health, Bethesda, Maryland, USA). To assess eNOS dimer formation, non-denaturing low-temperature SDS-PAGE was employed. Aortas were lysed as described above, treated with 6x Laemmli`s buffer not containing β-mercaptoethanol, and immediately subjected to 6% SDS-PAGE without prior incubation at 99°C.

eNOS s-glutathionylation

Twenty mg of aortic tissue were lysed in lysis buffer supplemented with 25mM N-ethylmaleimide (NEM) (Sigma-Aldrich). eNOS was immunoprecipitated at 4°C overnight with NOS3 (C-20) agarose-conjugated antibody (Santa Cruz Biotechnology, Dallas, Texas, USA), eluted by two 10min 50°C 500rpm incubations with non-reducing 6xLaemmli`s buffer supplemented with 25mM NEM, and immediately subjected to non-reducing SDS-PAGE. S-glutathione was detected using anti-glutathione antibody (Virogen, Watertown, MA, USA) supplemented with 2.5mM NEM, and anti-eNOS/NOS Type III antibody (BD Biosciences).

DHE staining on rats aortae

Frozen 10 μm sections from aortae were cut with a Leica CM3050S cryostat and placed on positive-charged slides (Superfrost Plus, Thermo Scientific, Waltham, MA, USA). Dihydroethidium (Sigma Aldrich) was prepared as stock solution in DMSO, diluted in deoxygenated PBS (final concentration 5μM), and applied to frozen sections for 30 min at 37°C. Nuclei were counterstained with Hoechst 33258 (Sigma Aldrich, final concentration 1μg/ml). Slides were coverslipped and images taken on a SP8 microscope (10x/0.30 objective; Leica, Solms, Germany), and quantified (ImageJ, NIH). DHE fluorescence was calculated by subtracting the autofluorescence signal (green channel) from the DHE signal (red channel), and normalized to the total fluorescent area.

NADPH oxidase activity

NADPH oxidase activity was measured using a commercial NADP/NADPH assay kit (Abcam) according to the manufacturer`s instructions. To measure the effect of HDL on endothelial NADPH oxidase activity, HAECs were treated with HDL (50ug/ml) for one hour at 37°C, as described[7].

Serum bile acid measurements

Serum bile acids were measured with Cobas Integra 800 (Roche, Basel, Switzerland).

Plasma insulin and GLP-1 measurements

Customized rat and human duplex insulin/active GLP-1 Meso Scale Discovery 96-well plates were used to measure plasma insulin and GLP-1 concentrations, respectively, following the provided protocol (Meso Scale Discovery, Gaithersburg. MD, USA).

Serum HDL isolation by sequential density centrifugation

HDL was isolated from fresh, fasting plasma by density gradient ultracentrifugation (HDL: density 1.063 to 1.21 g/cm^3), as described[8, 9]. Potassium bromide (Merck KGaA, Darmstadt, Germany) was used to adjust the density. Purity of HDL was assessed by SDS-PAGE and subsequent Coomassie Blue staining of the gel.

Cell culture

Human aortic endothelial cells (HAEC) were obtained from (Lonza, Basel, Switzerland) and cultured in endothelial cell basal medium-2 (Lonza) supplemented with endothelial growth medium–SingleQuots as indicated by the manufacturer (37°C, 95% air / 5% CO2). HAECs were grown to sub-confluency and rendered quiescent before experiments by incubation in medium containing 0.5% fetal calf serum. For reverse cholesterol transport experiments, the murine macrophage cell line J774 was cultured on 75-cm2 flasks, in 10% FBS, 4.5g/l glucose RPMI medium 1640 (GIBCO, Life Technologies, Grand Island, NY, USA).

TNF α- induced VCAM 1 expression in HAEC stimulated with HDL

Expression of vascular cell adhesion molecule 1 (VCAM-1) was assessed in HAEC (passage 7-9) stimulated with TNF-α on 96-well black-wall clear-bottom plates (BD). HAECs were rendered quiescent before experiments and treated overnight with or without HDL (10-µg protein/mL), followed by four hours of stimulation with TNF-α (100pg/ml) before fixation. Blocking with Licor buffer and incubating cells with VCAM 1 (R&D Systems, Minneapolis, MN, USA). Washing and adding secondary antibody, anti-goat 800CW (green) with Draq-5 for normalization (680CW). For measurements the quantitative fluorescent imaging systems (LI-COR Odissey, Lincoln, Nebraska, USA) in channel 700CW and 800CW was used.

Measurement of endothelial cell NO production by 4,5-diaminofluorescein diacetate (DAF-2) staining.

Endothelial cell NO production was determined as described[10]. In brief, after overnight starvation HAEC were incubated for one hour at 37°C with HDL (60 μg/ml) and DAF-2 diacetate (1 μM; Cayman Chemical, Ann Arbor, Michigan, USA), that forms the fluorescent triazolofluorescein upon reaction with cellular NO. Following incubation, cells were transferred to a black microplate and fluorescence was measured on a Tecan Infinite M200 PRO reader (Tecan, Maennedorf, Switzerland) with excitation and emission wavelenghts of 485nm and 535nm, respectively.

Measurement of aortic NO production.

NO release in rat aortas was examined by electron spin resonance ESR spectroscopy analysis with the use of the spin-trap colloid Fe (DETC) 2 (Noxygen, Elzach, Germany), as described and validated previously[11, 12]. Briefly, Krebs-HEPES buffer (37°C), 500 μL of FeSO4 and DETC solution were added to each sample and incubated at 37°C for 60 minutes. Samples were frozen immediately in liquid nitrogen till recording with the use of NOX-E.5-ESR spectrometer (Bruker, Bremen, Germany). Signals were quantified by measuring the total amplitude after correction of baseline and subtraction of background signals.

PON-1 activity

Paraoxonase-1 (PON1) activity was determined using spectrophotometric measurement of rate of cleavage of phenylacetate (Sigma-Aldrich) to produce phenol in serum by monitoring the increase in absorbance at 270 nm at 25 °C, as described[13]. The resulting phenol concentration was calculated by the molar extinction coefficient, ε = 1,310 M–1 (pH 8.0). Each sample was run in duplicate. Activity of paraoxonase is expressed as umol/min/L.

In vitro apoptosis assay

HDL anti-apoptotic properties were assessed in HAEC by evaluating cytoplasmic DNA-histone complexes that increase after apoptosis associated DNA fragmentation, using the Cell Death Detection ELISA^{Plus} kit (Roche Biochemicals) according to the manufacturer's instructions.

In vitro reverse cholesterol transport capacity of HDL

J774 murine macrophages were seeded at a density of $1x10^6$ /well in 24-well plates and the next day labeled with 2 µCi/mL ^{3}H cholesterol for a minimum of 17 hours overnight in the presence of 2ug/ml acetyl-Coenzyme A acetyltransferase inhibitor (58-035, Sandoz Holzkirchen, Germany) in 500ul 0% FBS, 4.5g/l glucose RPMI 1640 medium (GIBCO, Life Technologies). The following day cells were washed 2x with PBS and equilibrated for six hours with 0.3mM 8-(4-bromophenylthio)-3'-5'-cyclic adenosine monophosphate (Sigma-Aldrich) in the presence of acetyl-Coenzyme A acetyltransferase inhibitor in 500ul 0% FBS 4.5g/l glucose RPMI medium. Apo B-depleted serum was obtained by polyethylene glycol precipitation, and 2.8% v/v Apo B-depleted serum was used as efflux acceptor for four hours in the presence of acetyl-Coenzyme A acetyltransferase inhibitor in 500ul 0% FBS MEM-25mM HEPES medium. As controls, 2.8% v/v Apo B-depleted healthy human serum or MEM-HEPES medium alone were used. Supernatants were collected and centrifuged during five minutes at 12 000 rpm and 250ul were used for ten minutes of liquid scintillation measurements (PerkinElmer, Boston, MA;USA). Cells were washed 1x with PBS and intracellular cholesterol was extracted twice sequentially with 500ul 3:2 hexane:isopropanol for thirty minutes and fifteen minutes respectively, evaporated under a N_2 flux and resuspended in 500ul isopropanol, from which 250ul were used for ten minutes liquid scintillation. Reverse cholesterol transport capacity of HDL was calculated as the ratio

between DPM counts of the supernatant vs. the intracellular ^{3}H cholesterol scintillation measurements.

Lipoprotein fractions

To assess the distribution of cholesterol over the different lipoprotein fractions, lipoproteins were separated by size exclusion chromatography followed by online determination of lipids[14] or by fast protein liquid chromatography (FPLC) using two Superose-6 FPLC columns in series (HR10/30) in PBS with 0.1 mM EDTA, pH 7.5 at 0.5 ml/min. Columns were calibrated using high and low molecular weight standards (Pharmacia, Stockholm, Sweden). 500 ul of serum was loaded on the column, the first 10 ml were discarded and afterwards 70 samples of 500 ul were collected for analysis. Cholesterol concentrations were measured using colorimetric and enzymatic methods with ready to use kits (Amplex red cholesterol kit, Life Technologies).

Patient population

Studies were performed according to the principles of the Declaration of Helsinki. The Local Research and Ethics committee approved the study (KEK-ZH-Nr. 2012-0260), and all patients gave written consent. The surgery group consisted of 29 patients undergoing primary laparoscopic proximal RYGB surgery. The RYGB procedure was performed as described[15]. All patients underwent a clinical, biochemical and pre-anesthetic evaluation, and all patients adhered to the study protocol and completed follow-up. Patients with unstable medical conditions such as recent coronary syndromes (within six months), congestive heart failure, systemic infection, acute illness, malignancy, or pregnancy, substance abuse, more than three alcoholic drinks per day, or psychiatric illness were excluded. Fasting blood samples were collected before (D0), at the first outpatient appointment two weeks (D14), and 12 weeks

(W12) post RYGB surgery. The BMI-matched group consisted of 29 obese patients, who were asymptomatic with no history of heart disease and not undergoing any cardiovascular conditioning program.

The BMI, body weight, age and gender of these patients were matched to the BMI of patients 12 weeks after RYGB. The control group consisted of 28 normal-weight volunteers matched for age and sex. They did not undergo any cardiovascular conditioning program. All control subjects were asymptomatic with no history of heart disease or accompanying disorders.

Blood sampling

Blood samples were obtained from fasting patients before RYGB (D0), in the morning of the first outpatient appointment two weeks after RYGB surgery (D14), and 12 weeks (W12) post RYGB surgery. Serum was collected in non-additive vacutainers, and plasma was collected in BD P800 vacutainers (containing DPPIV and protease inhibitors) that were kept at +4°C before and after blood collection. Blood samples were collected from fasting healthy subjects at the time of the study enrollment; plasma and serum were processed as described above.

Statistical Analysis

All analyses were performed with GraphPad Prism Software (version 5.0) or with SPSS software version 22.0 (Chicago, SPSS, Inc., Chicago, Illinois, USA).

Supplementary Results

RYGB reduces Food Intake and Body Weight compared to sham-operated controls

In the first experiment, RYGB reduced food intake (FI) and body weight relative to sham-operated *ad libitum* fed rats (controls) (SOM, Fig. 3 A-B). The body weight of the weight-

matched group was well matched to RYGB rats, thus allowing the discrimination of surgery-specific from weight-dependent effects since the only variable between these two study groups was the RYGB procedure. In the second experiment, FI and body weight were decreased to a similar extent in vehicle-treated RYGB versus sham-operated rats. Exendin$_{9\text{-}39}$ treatment in RYGB rat did not affect food intake or weight compared to the vehicle-treated RYGB (SOM, Fig. 3 C-D). Sham operated controls rats receiving liraglutide ate less initially, but they progressively increased their FI to a level similar to sham-operated controls on day 5 after surgery. The initial weight decrease in liraglutide-treated sham-operated rats was similar to that in RYGB rats, but liraglutide-treated rats started to regain some weight three to four days after treatment onset, as described[16] (SOM Fig.3 C-D). Some sham-operated and RYGB rats were followed up for one month in order to assess prolonged changes and compare weight-dependent effects (RYGB vs controls) with weight-independent effects (RYGB vs weight-matched). Sham-operated controls ate more compared to RYGB and weight-matched rats. The body weight of RYGB and weight-matched was well matched and remained stable around 470g after the initial weight loss (SOM Fig. 3 E-F).

The improvement of vascular function after RYGB is weight-independent.

Aortic contractions after norepinephrine (NE) were similar in sham-operated or RYGB rats (data not shown) in all experiments. Endothelium-independent relaxations in response to sodium nitroprusside (SNP) were equally preserved eight days after surgery (SOM Fig.4 C, H). Interestingly, one month after surgery, RYGB maintained a better relaxation in response to both insulin and GLP-1 with respect to sham-operated rats, whereas, acetylcholine-induced relaxation was restored in weight-matched equally to RYGB rats (SOM Fig. 4 D-F). Hence, although their weight was reduced as in the RYGB, weight-matched rats did not improve their relaxation upon stimulation with both hormones Because the response to acetylcholine one

month after surgery was similar in weight-matched and RYGB, insulin and GLP-1 are likely to be a more sensitive tools to investigate vascular function than muscarinic receptor-induced relaxation in this model of HFHC-induced obesity. After one month, endothelium-independent relaxations to sodium nitroprusside (SNP) (10^{-10}–10^{-5} mol/L) were similar in all groups (data not shown).

Improved HDL profile after RYGB

Despite similar plasmatic HDL-cholesterol concentrations among the study groups (SOM Fig 6 A), the analysis of the cholesterol distribution profile across all fast protein liquid chromatography (FPLC)-separated lipoprotein fractions revealed a clear shift towards smaller size and more uniformed HDL particle after RYGB (SOM Fig 6 B-C). The cholesterol distribution profile attributed to the HDL particles in sham-operated rats was similar to what has been described in animals fed high cholesterol diets[17]. Notably, sham-operated controls treated with liraglutide exhibited cholesterol attributed to smaller HDL particles similar to RYGB, whereas the absence of effect after exendin$_{9\text{-}39}$ compared to RYGB advocates an action independent of the classical GLP-1 receptor (SOM Fig.6 D).

Patient characteristics and follow-up after RYGB

The anthropometric characteristics, medications and lipid profile of obese patients undergoing RYGB surgery and those of the group BMI-matched to week 12 after RYGB are presented in SOM Table 1. All patients adhered to the study protocol and completed follow-up. The mean preoperative BMI was 45.44±1.0 kg/m2, n= six patients were super-obese (BMI> 50kg/m2). As expected, there was a high prevalence of obesity associated comorbidities at the time of study enrollment; T2DM was present in 20%; hypertension in 33% and obstructive sleep

apnea (OSAS) in 31% of the patients. There were five (17%) current smokers. At D14, the acute phase reaction post-surgical trauma was resolved as confirmed by the post-operative time course of IL-6, C-reactive protein (CRP) levels and leukocyte counting (data not shown); weight and BMI were reduced (42.20±1.0) (SOM Table 1), and decreased further at W12 (weight loss= 18.2%; mean BMI 37.13 kg/m2). RYGB patient at baseline had significantly lower concentrations of HDL-C and higher concentrations of TG than controls. Postoperative changes of HDL-C followed a U shaped curve: there was a significant decrease from baseline to D14 followed by an increase at 12 weeks, but HDL-C was lower than in controls. Triglycerides levels improved by RYGB but remained higher than in controls, even 12 weeks after RYGB; these levels were lower 12 weeks after surgery than in the BMI-matched group. As expected, age-matched, healthy subjects significantly differed from obese with respect to weight and BMI. As shown in SOM Table 2, RYGB was associated with a significant increase in fasting circulating GLP-1 and bile acids levels paralleled by a significant decrease in glucose, insulin levels and in Homeostatic model assessment for insulin resistance (HOMA).

References

1. Bueter M, Abegg K, Seyfried F, Lutz TA, le Roux CW. Roux-en-y gastric bypass operation in rats. *J Vis Exp*. 2012:e3940
2. Gaspari T, Liu H, Welungoda I, Hu Y, Widdop RE, Knudsen LB, Simpson RW, Dear AE. A glp-1 receptor agonist liraglutide inhibits endothelial cell dysfunction and vascular adhesion molecule expression in an apoe-/- mouse model. *Diab Vasc Dis Res*. 2011;8:117-124
3. Noyan-Ashraf MH, Shikatani EA, Schuiki I, Mukovozov I, Wu J, Li RK, Volchuk A, Robinson LA, Billia F, Drucker DJ, Husain M. A glucagon-like peptide-1 analog reverses the molecular pathology and cardiac dysfunction of a mouse model of obesity. *Circulation*. 2013;127:74-85
4. Mells JE, Fu PP, Sharma S, Olson D, Cheng L, Handy JA, Saxena NK, Sorescu D, Anania FA. Glp-1 analog, liraglutide, ameliorates hepatic steatosis and cardiac hypertrophy in c57bl/6j mice fed a western diet. *Am J Physiol Gastrointest Liver Physiol*. 2012;302:G225-235
5. Rask-Madsen C, Li Q, Freund B, Feather D, Abramov R, Wu IH, Chen K, Yamamoto-Hiraoka J, Goldenbogen J, Sotiropoulos KB, Clermont A, Geraldes P, Dall'Osso C, Wagers AJ, Huang PL, Rekhter M, Scalia R, Kahn CR, King GL. Loss of insulin signaling in vascular endothelial cells accelerates atherosclerosis in apolipoprotein e null mice. *Cell Metab*. 2010;11:379-389

6. Osto E, Matter CM, Kouroedov A, Malinski T, Bachschmid M, Camici GG, Kilic U, Stallmach T, Boren J, Iliceto S, Luscher TF, Cosentino F. C-jun n-terminal kinase 2 deficiency protects against hypercholesterolemia-induced endothelial dysfunction and oxidative stress. *Circulation*. 2008;118:2073-2080
7. Sorrentino SA, Besler C, Rohrer L, Meyer M, Heinrich K, Bahlmann FH, Mueller M, Horvath T, Doerries C, Heinemann M, Flemmer S, Markowski A, Manes C, Bahr MJ, Haller H, von Eckardstein A, Drexler H, Landmesser U. Endothelial-vasoprotective effects of high-density lipoprotein are impaired in patients with type 2 diabetes mellitus but are improved after extended-release niacin therapy. *Circulation*. 2010;121:110-122
8. Riwanto M, Rohrer L, Roschitzki B, Besler C, Mocharla P, Mueller M, Perisa D, Heinrich K, Altwegg L, von Eckardstein A, Luscher TF, Landmesser U. Altered activation of endothelial anti- and proapoptotic pathways by high-density lipoprotein from patients with coronary artery disease: Role of high-density lipoprotein-proteome remodeling. *Circulation*. 2013;127:891-904
9. Besler C, Heinrich K, Rohrer L, Doerries C, Riwanto M, Shih DM, Chroni A, Yonekawa K, Stein S, Schaefer N, Mueller M, Akhmedov A, Daniil G, Manes C, Templin C, Wyss C, Maier W, Tanner FC, Matter CM, Corti R, Furlong C, Lusis AJ, von Eckardstein A, Fogelman AM, Luscher TF, Landmesser U. Mechanisms underlying adverse effects of hdl on enos-activating pathways in patients with coronary artery disease. *J Clin Invest*. 2011;121:2693-2708
10. Leikert JF, Rathel TR, Muller C, Vollmar AM, Dirsch VM. Reliable in vitro measurement of nitric oxide released from endothelial cells using low concentrations of the fluorescent probe 4,5-diaminofluorescein. *FEBS Lett*. 2001;506:131-134
11. Kleschyov AL, Munzel T. Advanced spin trapping of vascular nitric oxide using colloid iron diethyldithiocarbamate. *Methods Enzymol*. 2002;359:42-51
12. Khoo JP, Alp NJ, Bendall JK, Kawashima S, Yokoyama M, Zhang YH, Casadei B, Channon KM. Epr quantification of vascular nitric oxide production in genetically modified mouse models. *Nitric Oxide*. 2004;10:156-161
13. Bhattacharyya T, Nicholls SJ, Topol EJ, Zhang R, Yang X, Schmitt D, Fu X, Shao M, Brennan DM, Ellis SG, Brennan ML, Allayee H, Lusis AJ, Hazen SL. Relationship of paraoxonase 1 (pon1) gene polymorphisms and functional activity with systemic oxidative stress and cardiovascular risk. *JAMA*. 2008;299:1265-1276
14. Hesse D, Radloff K, Jaschke A, Lagerpusch M, Chung B, Tailleux A, Staels B, Schurmann A. Hepatic trans-golgi action coordinated by the gtpase arfrp1 is crucial for lipoprotein lipidation and assembly. *J Lipid Res*. 2014;55:41-52
15. Weber M, Muller MK, Bucher T, Wildi S, Dindo D, Horber F, Hauser R, Clavien PA. Laparoscopic gastric bypass is superior to laparoscopic gastric banding for treatment of morbid obesity. *Ann Surg*. 2004;240:975-982; discussion 982-973
16. Williams DL, Hyvarinen N, Lilly N, Kay K, Dossat A, Parise E, Torregrossa AM. Maintenance on a high-fat diet impairs the anorexic response to glucagon-like-peptide-1 receptor activation. *Physiol Behav*. 2011;103:557-564
17. Mahley RW, Weisgraber KH, Innerarity T, Brewer HB, Jr., Assmann G. Swine lipoproteins and atherosclerosis. Changes in the plasma lipoproteins and apoproteins induced by cholesterol feeding. *Biochemistry*. 1975;14:2817-2823

Supplementary Figure Legends

Figure 1.

Study design of the two main animal experiments (A) RYGB, sham-operated *ad libitum* fed (controls) or body weight- matched to RYGB rats followed up for eight days; (B) RYGB or sham-operated controls followed up for eight days with simultaneous *in vivo* pharmacological intervention.

Figure 2.

Plasma levels of GLP-1 (A) and total bile acids (B) in RYGB compared to sham-operated rats one month after surgery, (*RYGB vs controls and weight-matched, p=0.0001). Values are means ± SEM. n= 10-15 each group.

Figure 3.

A. Cumulative 24 hours-food intake in sham-operated controls (n=12), RYGB (n=17) and sham-operated weight-matched (n= 12) rats on the eight post-operative days. Average cumulative food intake was significantly higher in sham-operated controls vs. RYGB, and sham-operated weight-matched rats, (*** controls vs RYGB and weight-matched, p <0.001). No statistically significant difference was observed between RYGB and weight-matched rats.

B. Body weight before and eight days after surgery. Body weight was significantly higher in controls compared to RYGB rats starting from day 4; body weight did not differ between RYGB and weight-matched rats (*, **, *** controls vs RYGB; ° controls vs weight-matched, p<0.05, p<0.01, p<0.001, respectively). **C.** Cumulative 24 hours-food intake in controls (n=6), $controls_{\text{-liraglutide}}$ (n=6); RYGB (n=11), $RYGB_{\text{-exendin9-39}}$ (n=10). Average cumulative food intake was significantly higher in controls vs. RYGB and $RYGB_{\text{-exendin9-39}}$ rats (*, **, *** controls vs RYGB and $RYGB_{\text{-exendin9-39}}$; °,°°,°°° controls vs $controls_{\text{-liraglutide}}$, p

<0.05, p<0.01, p<0.001, resp.; § RYGB and RYGB$_{\text{-exendin9-39}}$ vs. controls$_{\text{-liraglutide}}$, p<0.05). There was no statistically significant difference between sham-operated controls and controls$_{\text{-liraglutide}}$ after post-operative day 5. **D.** Body weight increased progressively in sham-operated controls with statistically significant differences with RYGB$_{\text{-exendin9-39}}$ and RYGB (* controls vs RYGB and RYGB$_{\text{-exendin9-39}}$; p<0.05). **E.** Cumulative 24 hours-food intake in controls (n=12), RYGB (n=19) and sham-operated weight-matched (n= 12) rats during the 1 month postoperative period. Average cumulative food intake was significantly higher in sham-operated controls vs. RYGB, and weight-matched rats, (*** sham-operated controls vs RYGB and weight-matched, p <0.001). No statistically significant differences were observed between RYGB and weight-matched rats after surgery (°°RYGB vs weight-matched; p<0.01). **F.** Body weight after one month was significantly higher in controls rats compared to RYGB and sham-operated weight-matched (*** controls vs RYGB and weight-matched, p <0.001; °controls vs. RYGB, p<0.05). Results are presented as means ± SEM.

Figure 4.

A-C Endothelium-dependent relaxation (during submaximal contraction to norepinephrine (NE)) of aortic rings isolated eight days after RYGB compared to sham-operated rats (A) concentration-response curves in response to GLP-1 in the presence of the highly specific GLP-1 receptor antagonist exendin$_{9\text{-}39}$ (10^{-5} mol/l, 10 min before GLP-1). (B) Line graphs show concentration-response curves to acetylcholine (Ach). (C) Endothelium-independent relaxation to the NO donor sodium nitroprusside (SNP) across the experimental groups (*sham-operated controls rats vs RYGB; ° sham-operated weight-matched vs. RYGB, p<0.05).

D-F Endothelium-dependent relaxation one month after RYGB compared to sham-operated rats in response to insulin (D), GLP-1 (E) and (F) to acetylcholine (Ach) (*controls rats vs RYGB; ° weight-matched vs RYGB rats; § controls vs weight-matched, p<0.05 respectively).

G-H Effects of eight days treatment with liraglutide or exendin$_{9\text{-}39}$ in sham-operated controls and RYGB, respectively, on endothelium-dependent (G) relaxation to Ach and endothelium-independent response to SNP (H) (*sham-operated controls vs RYGB, $p<0.05$). Results are presented as means ± SEM. n=6 to 8 per group.

I-N Concentration-response curves in response to insulin and GLP-1 in the presence of the free radical scavenger polyethylene glycol–superoxide dismutase (SOD 150 U/mL) of aortic rings isolated eight days after RYGB and after GLP-1 modulation (* RYGB vs. sham-operated weight-matched; # controls vs. controls$_{\text{-liraglutide}}$; § controls vs. RYGB$_{\text{-exendin9-39}}$, $p<0.05$). Results are presented as means ± SEM. n=6 to 8 per group.

Figure 5.

(A-B) GSH immunoblotting of eNOS immunoprecipitated from rat aortae eight days after RYGB and after GLP-1 modulation (* RYGB vs. sham-operated weight-matched; $p<0.01$).

Figure 6.

HDL associated PON-1 activity. (A) Eight days after RYGB and after GLP-1 modulation (C). HDL-stimulated cholesterol efflux in J774 macrophages (as % of sham-operated controls); eight days after RYGB (B) and after GLP-1 modulation (D). (* RYGB vs. other groups; # sham-operated controls$_{\text{-liraglutide}}$ vs RYGB; ° sham-operated controls vs RYGB$_{\text{-exendin9-39}}$, $p<0.05$). Results are presented as means ± SEM n=8-10 in each group.

Figure 7.

The abnormal HDL particles size induced by high fat high cholesterol diet is reversed after RYGB and liraglutide treatment. Total HDL-cholesterol levels eight days after RYGB were unchanged (A). Cholesterol distribution profile across all fast protein liquid chromatography

(FPLC)-separated lipoprotein fractions from samples isolated eight days (B) and one month after surgery (C) and after liraglutide or exendin$_{9-39}$ treatment in sham-operated controls or RYGB rats, respectively (D). Results are presented as means ± SEM; n=5-7 per group.

References to supplementary material

1. Bueter M, Abegg K, Seyfried F, Lutz TA, le Roux CW. Roux-en-y gastric bypass operation in rats. *J Vis Exp*. 2012:e3940
2. Gaspari T, Liu H, Welungoda I, Hu Y, Widdop RE, Knudsen LB, Simpson RW, Dear AE. A glp-1 receptor agonist liraglutide inhibits endothelial cell dysfunction and vascular adhesion molecule expression in an apoe-/- mouse model. *Diab Vasc Dis Res*. 2011;8:117-124
3. Noyan-Ashraf MH, Shikatani EA, Schuiki I, Mukovozov I, Wu J, Li RK, Volchuk A, Robinson LA, Billia F, Drucker DJ, Husain M. A glucagon-like peptide-1 analog reverses the molecular pathology and cardiac dysfunction of a mouse model of obesity. *Circulation*. 2013;127:74-85
4. Mells JE, Fu PP, Sharma S, Olson D, Cheng L, Handy JA, Saxena NK, Sorescu D, Anania FA. Glp-1 analog, liraglutide, ameliorates hepatic steatosis and cardiac hypertrophy in c57bl/6j mice fed a western diet. *Am J Physiol Gastrointest Liver Physiol*. 2012;302:G225-235
5. Rask-Madsen C, Li Q, Freund B, Feather D, Abramov R, Wu IH, Chen K, Yamamoto-Hiraoka J, Goldenbogen J, Sotiropoulos KB, Clermont A, Geraldes P, Dall'Osso C, Wagers AJ, Huang PL, Rekhter M, Scalia R, Kahn CR, King GL. Loss of insulin signaling in vascular endothelial cells accelerates atherosclerosis in apolipoprotein e null mice. *Cell Metab*. 2010;11:379-389
6. Osto E, Matter CM, Kouroedov A, Malinski T, Bachschmid M, Camici GG, Kilic U, Stallmach T, Boren J, Iliceto S, Luscher TF, Cosentino F. C-jun n-terminal kinase 2 deficiency protects against hypercholesterolemia-induced endothelial dysfunction and oxidative stress. *Circulation*. 2008;118:2073-2080
7. Sorrentino SA, Besler C, Rohrer L, Meyer M, Heinrich K, Bahlmann FH, Mueller M, Horvath T, Doerries C, Heinemann M, Flemmer S, Markowski A, Manes C, Bahr MJ, Haller H, von Eckardstein A, Drexler H, Landmesser U. Endothelial-vasoprotective effects of high-density lipoprotein are impaired in patients with type 2 diabetes mellitus but are improved after extended-release niacin therapy. *Circulation*. 2010;121:110-122
8. Riwanto M, Rohrer L, Roschitzki B, Besler C, Mocharla P, Mueller M, Perisa D, Heinrich K, Altwegg L, von Eckardstein A, Luscher TF, Landmesser U. Altered activation of endothelial anti- and proapoptotic pathways by high-density lipoprotein from patients with coronary artery disease: Role of high-density lipoprotein-proteome remodeling. *Circulation*. 2013;127:891-904
9. Besler C, Heinrich K, Rohrer L, Doerries C, Riwanto M, Shih DM, Chroni A, Yonekawa K, Stein S, Schaefer N, Mueller M, Akhmedov A, Daniil G, Manes C, Templin C, Wyss C, Maier W, Tanner FC, Matter CM, Corti R, Furlong C, Lusis AJ, von Eckardstein A, Fogelman AM, Luscher TF, Landmesser U. Mechanisms underlying adverse effects of hdl on enos-activating pathways in patients with coronary artery disease. *J Clin Invest*. 2011;121:2693-2708
10. Leikert JF, Rathel TR, Muller C, Vollmar AM, Dirsch VM. Reliable in vitro measurement of nitric oxide released from endothelial cells using low concentrations of the fluorescent probe 4,5-diaminofluorescein. *FEBS Lett*. 2001;506:131-134
11. Kleschyov AL, Munzel T. Advanced spin trapping of vascular nitric oxide using colloid iron diethyldithiocarbamate. *Methods Enzymol*. 2002;359:42-51

12. Khoo JP, Alp NJ, Bendall JK, Kawashima S, Yokoyama M, Zhang YH, Casadei B, Channon KM. Epr quantification of vascular nitric oxide production in genetically modified mouse models. *Nitric Oxide*. 2004;10:156-161
13. Bhattacharyya T, Nicholls SJ, Topol EJ, Zhang R, Yang X, Schmitt D, Fu X, Shao M, Brennan DM, Ellis SG, Brennan ML, Allayee H, Lusis AJ, Hazen SL. Relationship of paraoxonase 1 (pon1) gene polymorphisms and functional activity with systemic oxidative stress and cardiovascular risk. *JAMA*. 2008;299:1265-1276
14. Hesse D, Radloff K, Jaschke A, Lagerpusch M, Chung B, Tailleux A, Staels B, Schurmann A. Hepatic trans-golgi action coordinated by the gtpase arfrp1 is crucial for lipoprotein lipidation and assembly. *J Lipid Res*. 2014;55:41-52
15. Weber M, Muller MK, Bucher T, Wildi S, Dindo D, Horber F, Hauser R, Clavien PA. Laparoscopic gastric bypass is superior to laparoscopic gastric banding for treatment of morbid obesity. *Ann Surg*. 2004;240:975-982; discussion 982-973
16. Williams DL, Hyvarinen N, Lilly N, Kay K, Dossat A, Parise E, Torregrossa AM. Maintenance on a high-fat diet impairs the anorexic response to glucagon-like-peptide-1 receptor activation. *Physiol Behav*. 2011;103:557-564
17. Mahley RW, Weisgraber KH, Innerarity T, Brewer HB, Jr., Assmann G. Swine lipoproteins and atherosclerosis. Changes in the plasma lipoproteins and apoproteins induced by cholesterol feeding. *Biochemistry*. 1975;14:2817-2823

Figure 1

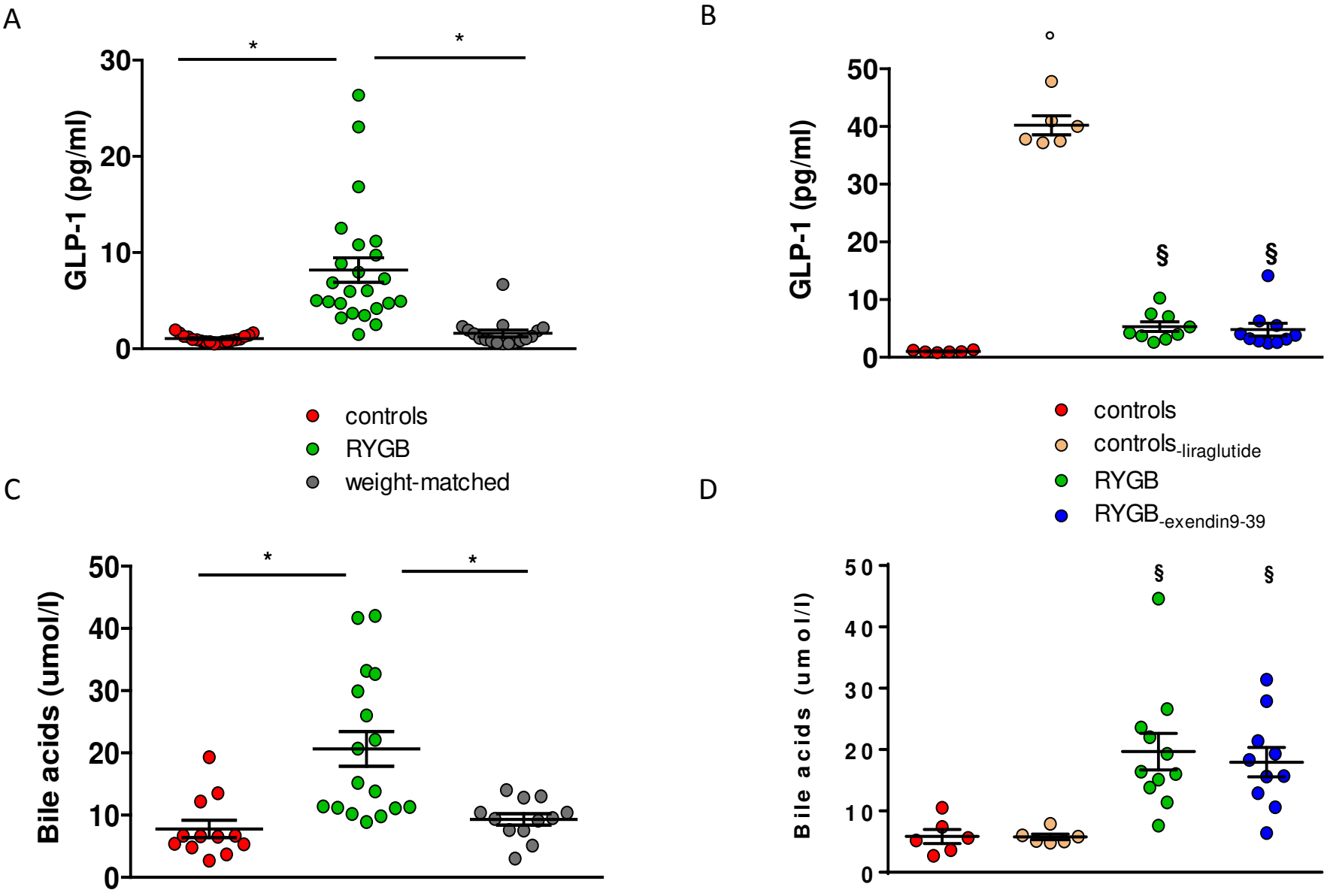
A
B
C
D
GLP-1 (pg/ml)
Bile acids (umol/l)
*
§
controls
RYGB
weight-matched
controls-liraglutide
RYGB-exendin9-39

Figure 2

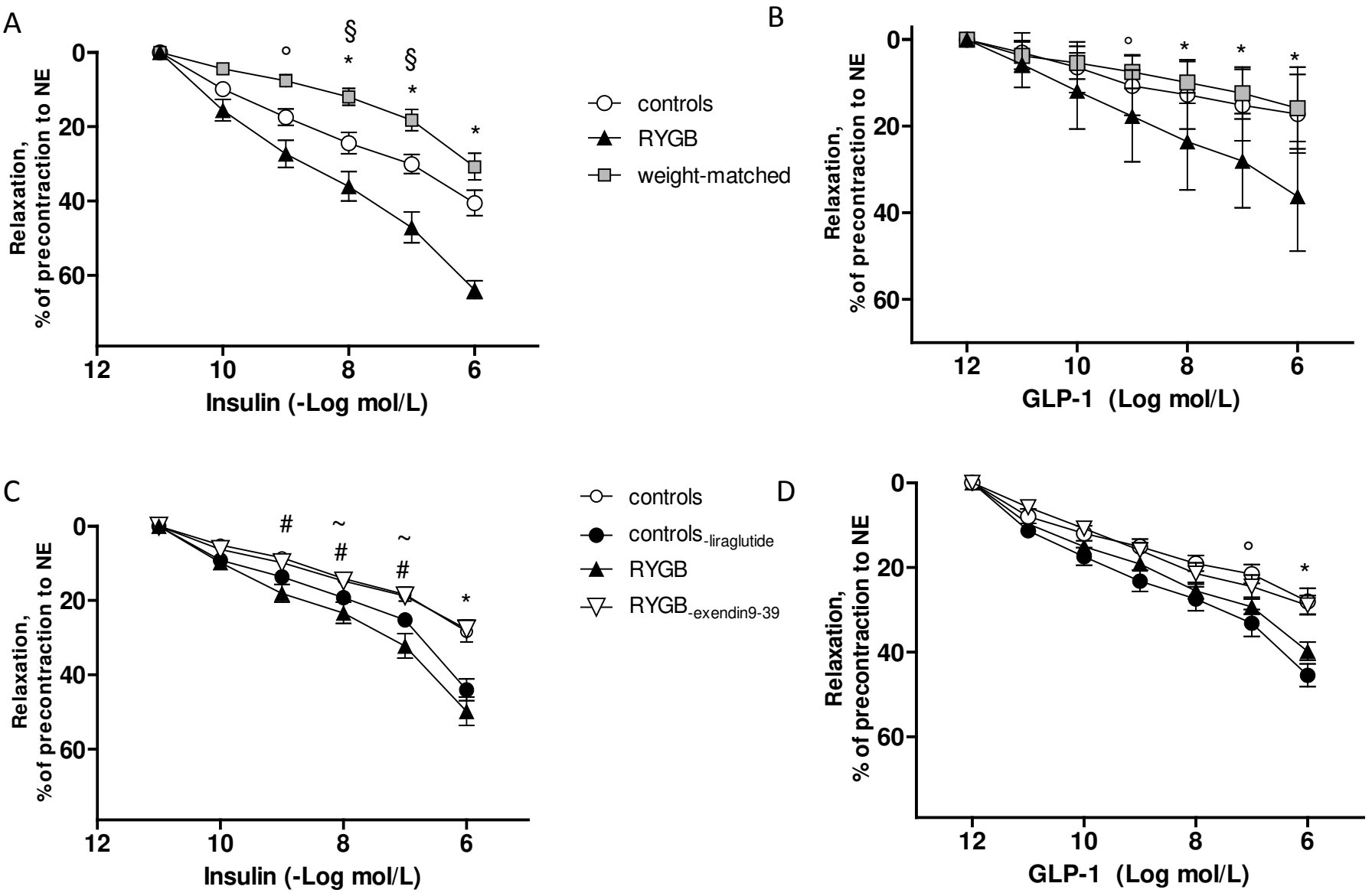
A
B
C
D
Relaxation, % of precontraction to NE
Insulin (-Log mol/L)
GLP-1 (Log mol/L)
controls
RYGB
weight-matched
controls-liraglutide
RYGB-exendin9-39
0
20
40
60
12
10
8
6
°
§
*
#
~

Figure 3

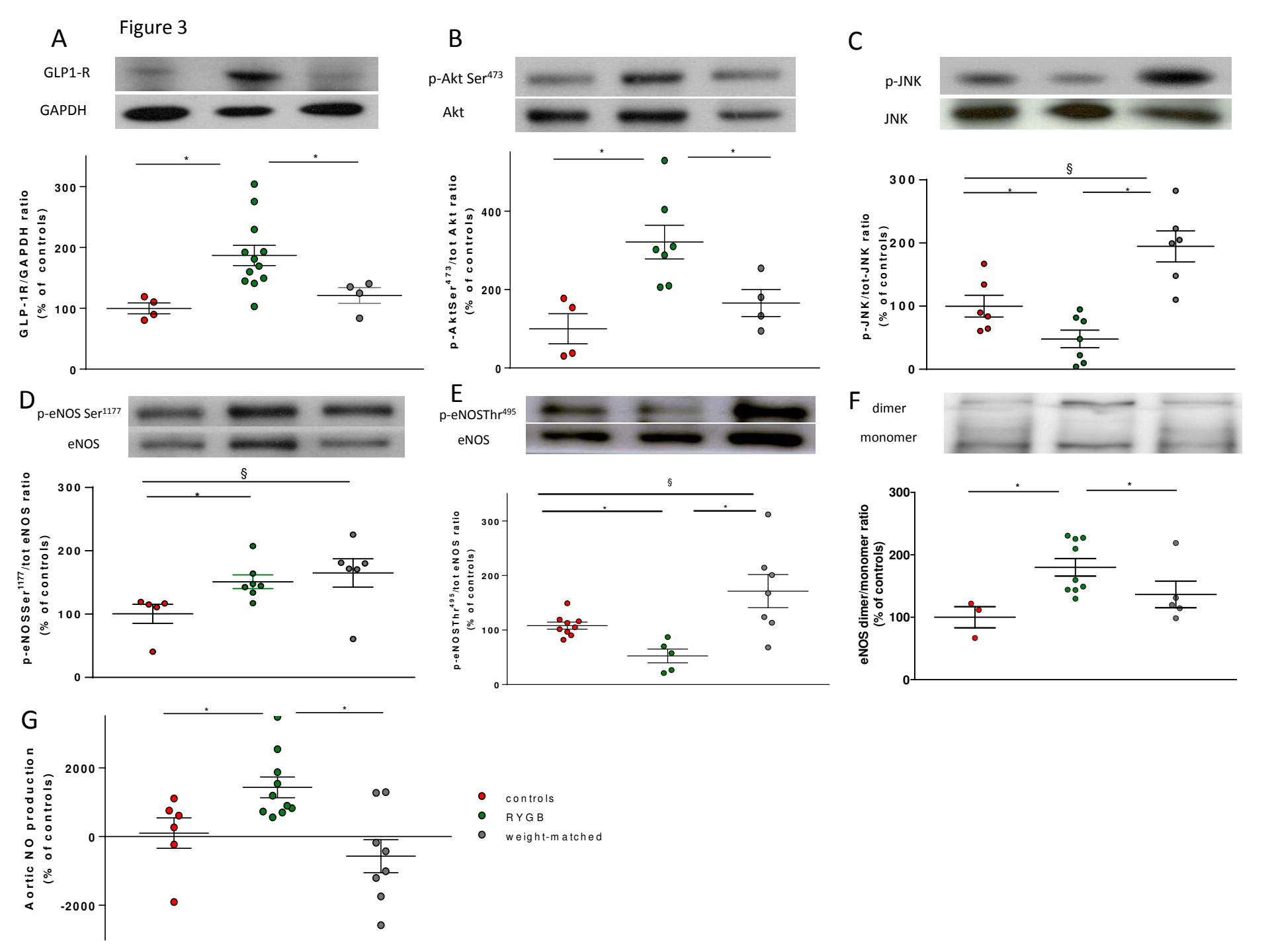
A
GLP1-R
GAPDH
GLP-1R/GAPDH ratio (% of controls)
B
p-Akt Ser473
Akt
p-AktSer473/tot Akt ratio (% of controls)
C
p-JNK
JNK
p-JNK/tot-JNK ratio (% of controls)
D
p-eNOS Ser1177
eNOS
p-eNOSSer1177/tot eNOS ratio (% of controls)
E
p-eNOSThr495
eNOS
p-eNOSThr495/tot eNOS ratio (% of controls)
F
dimer
monomer
eNOS dimer/monomer ratio (% of controls)
G
Aortic NO production (% of controls)
controls
RYGB
weight-matched

Figure 4

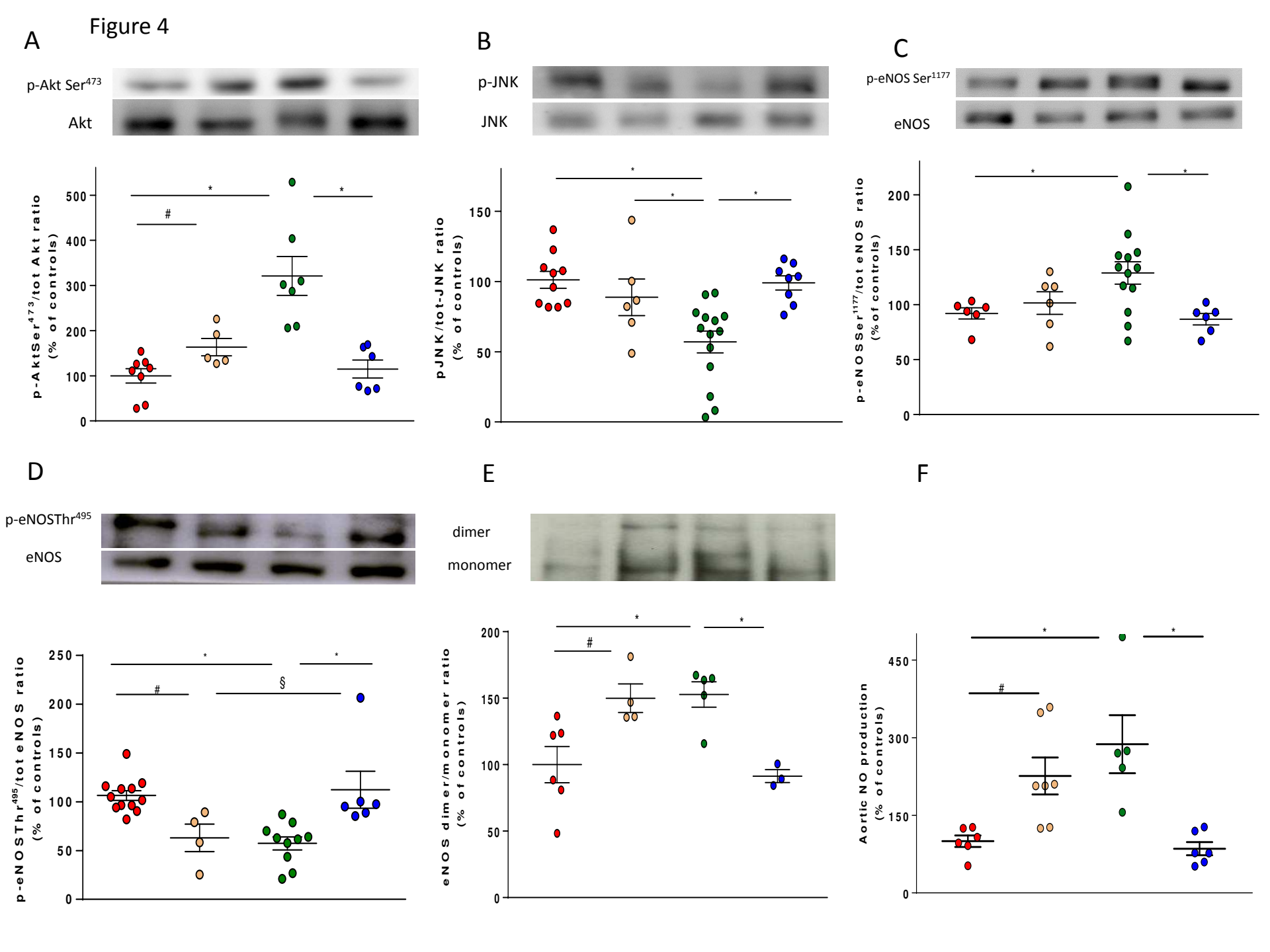
A
p-Akt Ser473
Akt
p-AktSer473/tot Akt ratio (% of controls)
B
p-JNK
JNK
pJNK/tot-JNK ratio (% of controls)
C
p-eNOS Ser1177
eNOS
p-eNOSSer1177/tot eNOS ratio (% of controls)
D
p-eNOSThr495
eNOS
p-eNOSThr495/tot eNOS ratio (% of controls)
E
dimer
monomer
eNOS dimer/monomer ratio (% of controls)
F
Aortic NO production (% of controls)

Figure 5

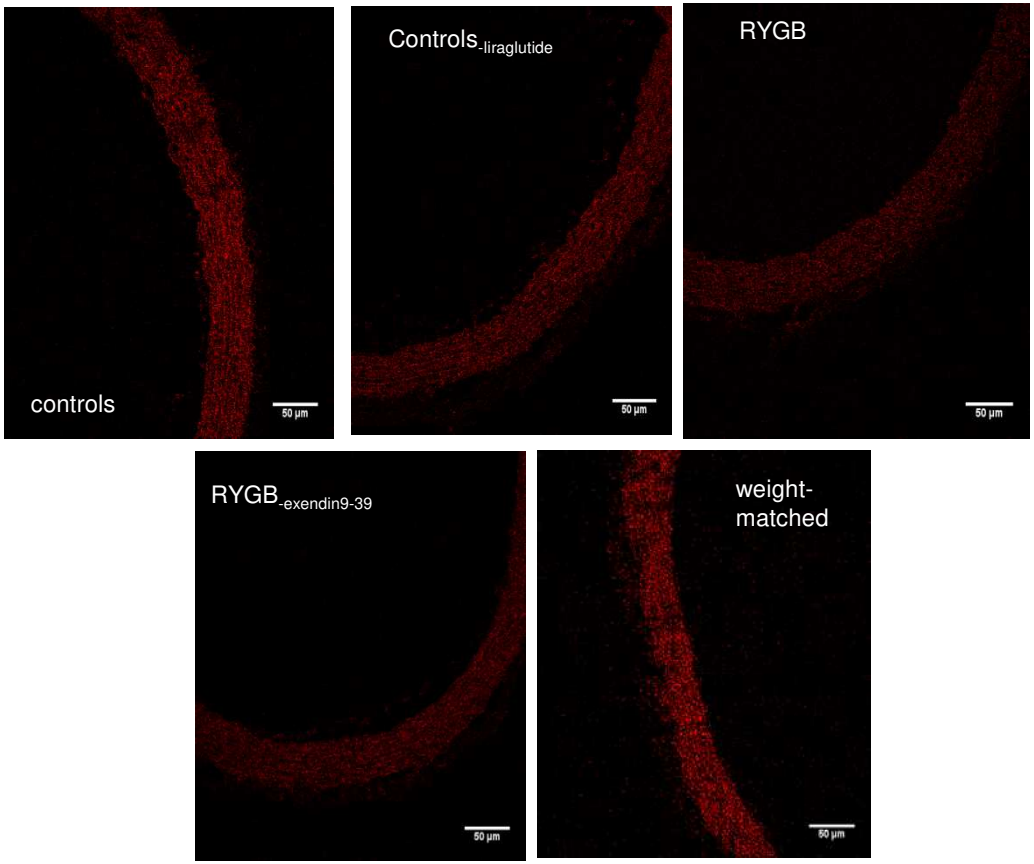
A
controls
Controls-liraglutide
RYGB
RYGB-exendin9-39
weight-matched
50 µm

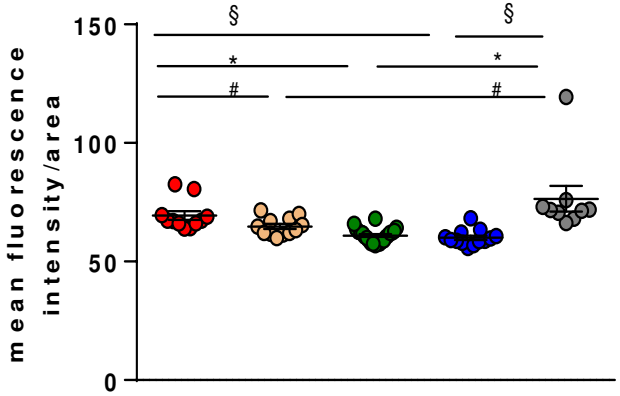
B
mean fluorescence intensity/area
150
100
50
0
§
*
#

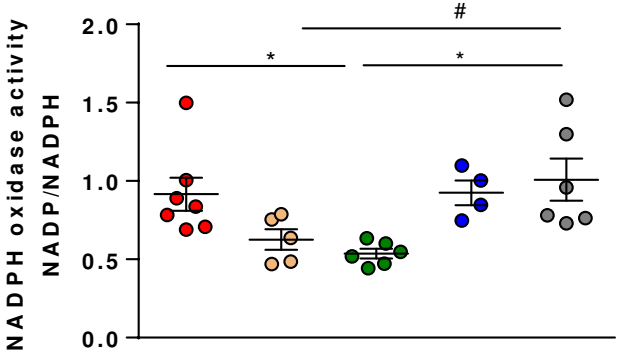
C
NADPH oxidase activity NADP/NADPH
2.0
1.5
1.0
0.5
0.0
*
#

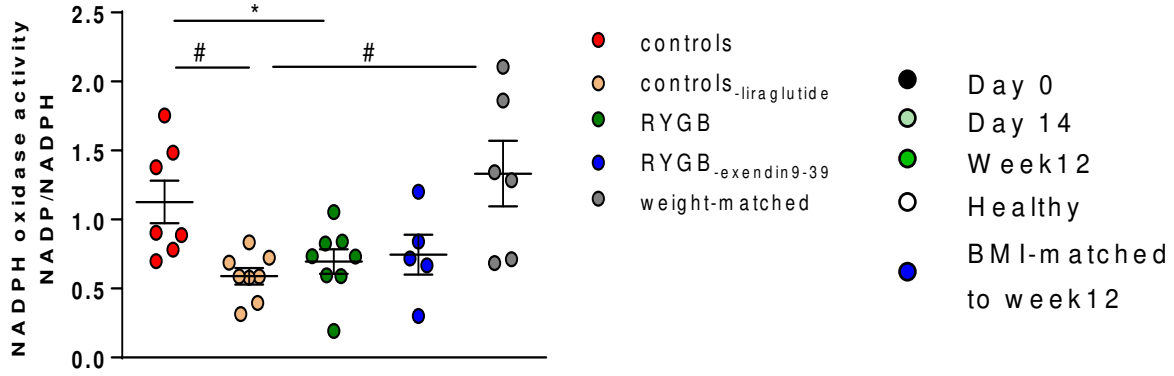
D
NADPH oxidase activity NADP/NADPH
2.5
2.0
1.5
1.0
0.5
0.0
*
#
controls
controls-liraglutide
RYGB
RYGB-exendin9-39
weight-matched

Day 0
Day 14
Week12
Healthy
BMI-matched to week12

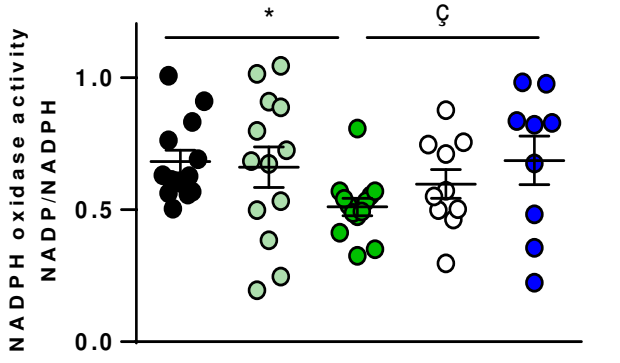
E
NADPH oxidase activity NADP/NADPH
1.0
0.5
0.0
*
Ç

Figure 6

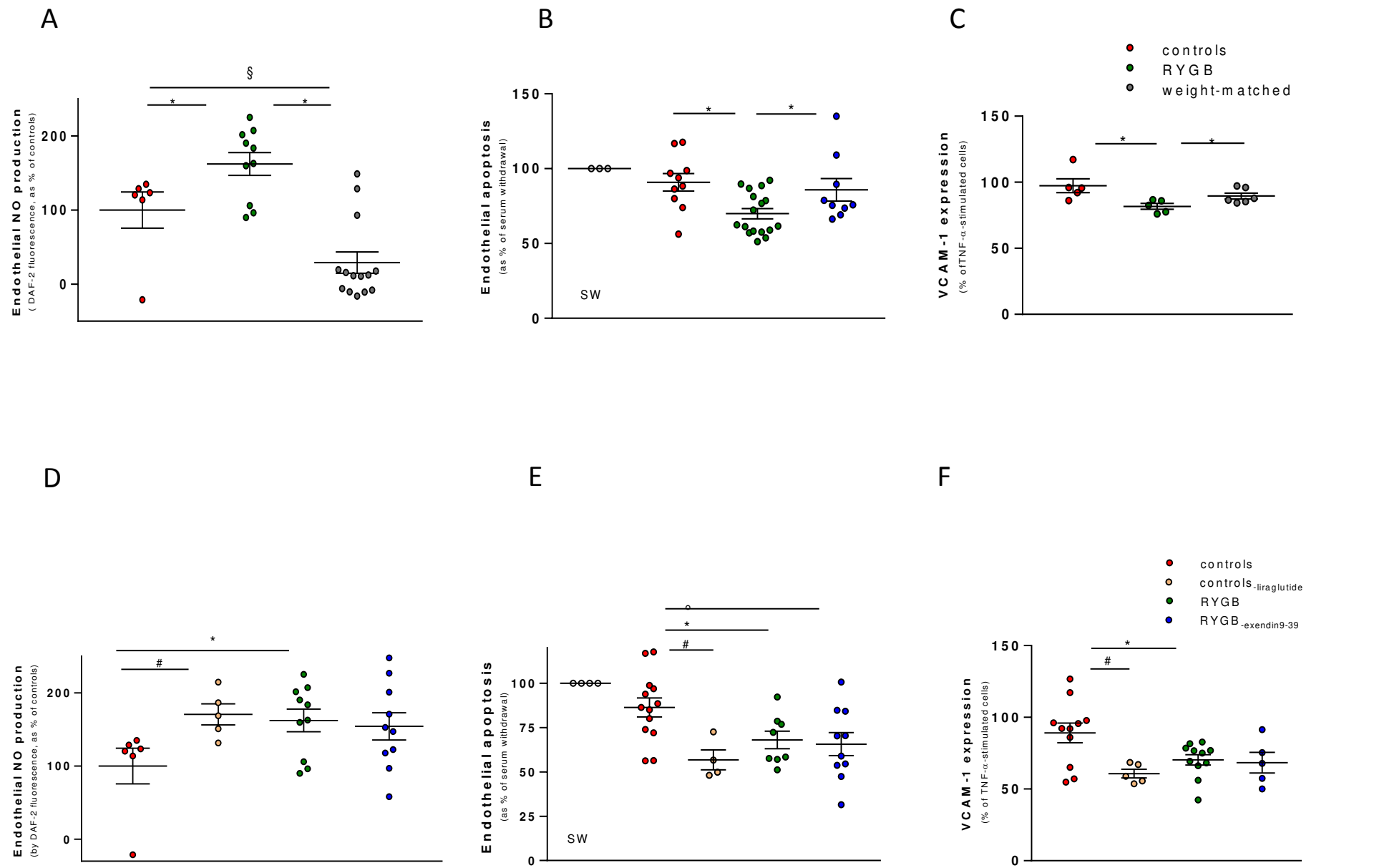
A
B
C
D
E
F
Endothelial NO production
(DAF-2 fluorescence, as % of controls)
Endothelial apoptosis
(as % of serum withdrawal)
SW
VCAM-1 expression
(% ofTNF-α-stimulated cells)
controls
RYGB
weight-matched
Endothelial NO production
(by DAF-2 fluorescence, as % of controls)
Endothelial apoptosis
(as % of serum withdrawal)
SW
VCAM-1 expression
(% of TNF-α-stimulated cells)
controls
controls-liraglutide
RYGB
RYGB-exendin9-39

Figure 7

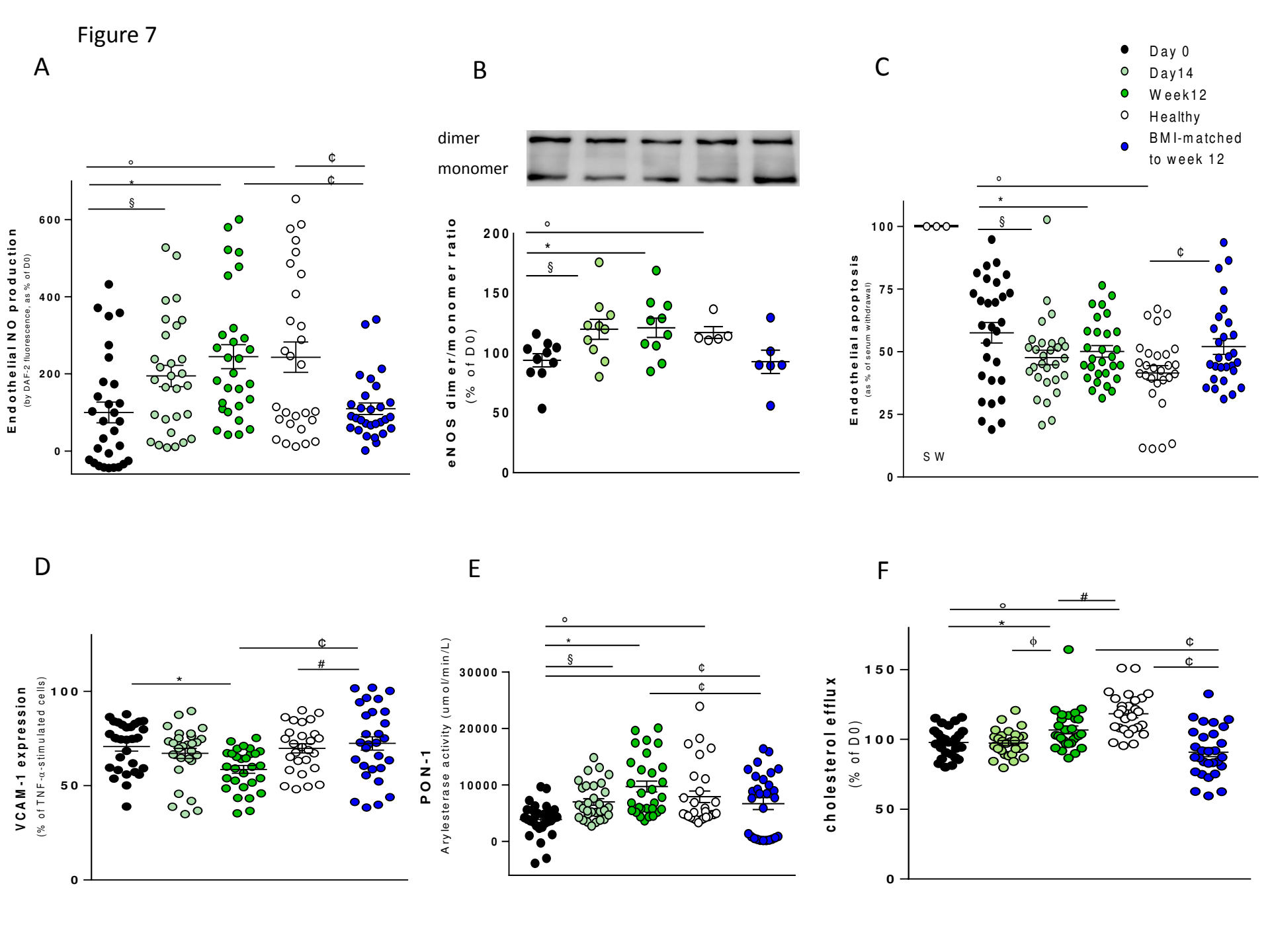
A
Endothelial NO production
(by DAF-2 fluorescence, as % of D0)
600
400
200
0
°
*
§
¢
¢
B
dimer
monomer
eNOS dimer/monomer ratio
(% of D0)
200
150
100
50
0
°
*
§
C
Day 0
Day14
Week12
Healthy
BMI-matched to week 12
Endothelial apoptosis
(as % of serum withdrawal)
100
75
50
25
0
°
*
§
¢
S W
D
VCAM-1 expression
(% of TNF-α-stimulated cells)
100
50
0
*
¢
#
E
PON-1
Arylesterase activity (umol/min/L)
30000
20000
10000
0
°
*
§
¢
¢
F
cholesterol efflux
(% of D0)
150
100
50
0
°
*
#
ϕ
¢
¢

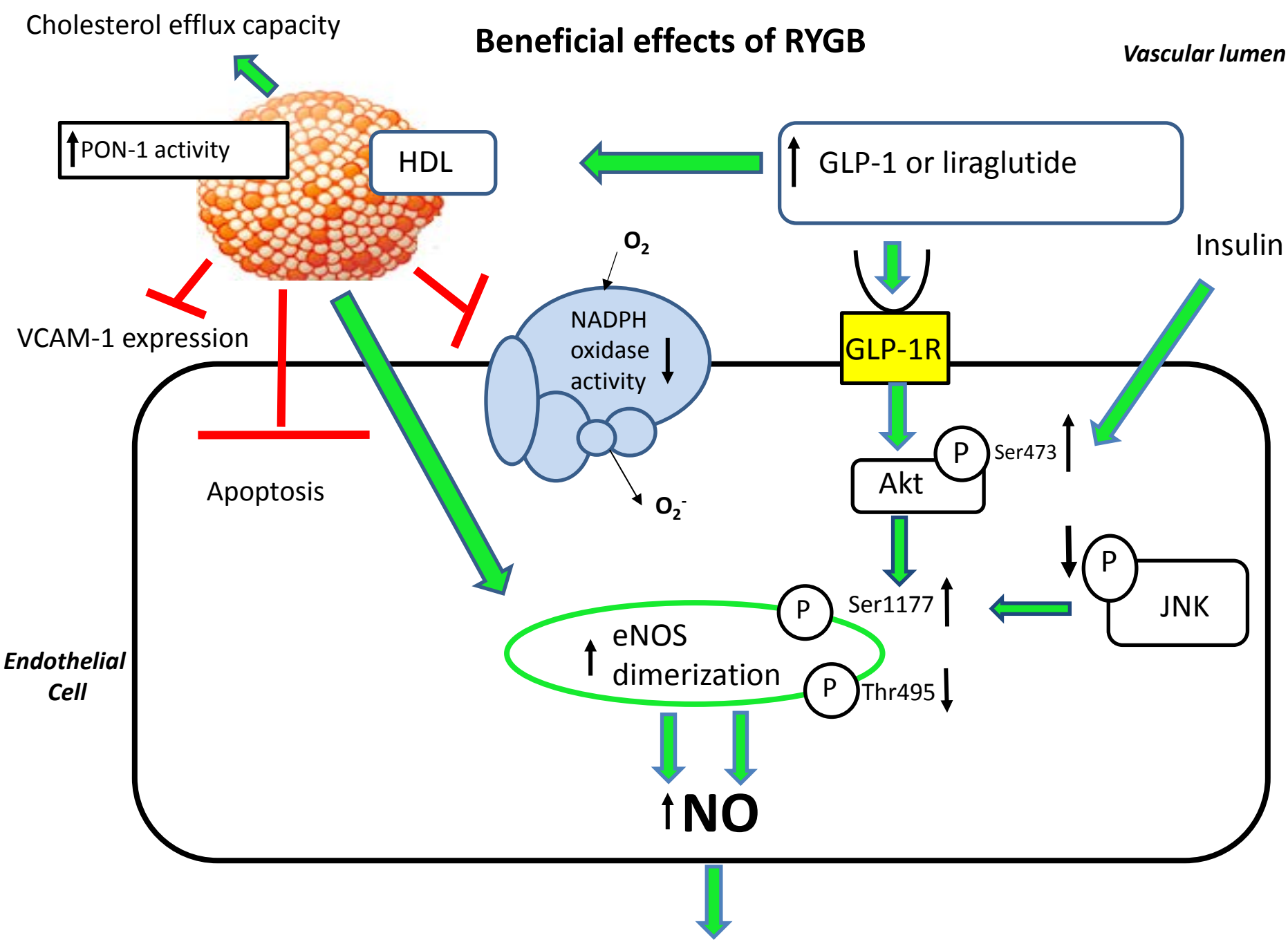
Cholesterol efflux capacity
Beneficial effects of RYGB
Vascular lumen
PON-1 activity
HDL
GLP-1 or liraglutide
Insulin
O_2
NADPH oxidase activity
O_2^-
GLP-1R
VCAM-1 expression
Apoptosis
P
Ser473
Akt
P
JNK
P
Ser1177
eNOS dimerization
P
Thr495
NO
Endothelial Cell
Improved endothelium-dependent relaxation

Figure 8

SOM Figure 1

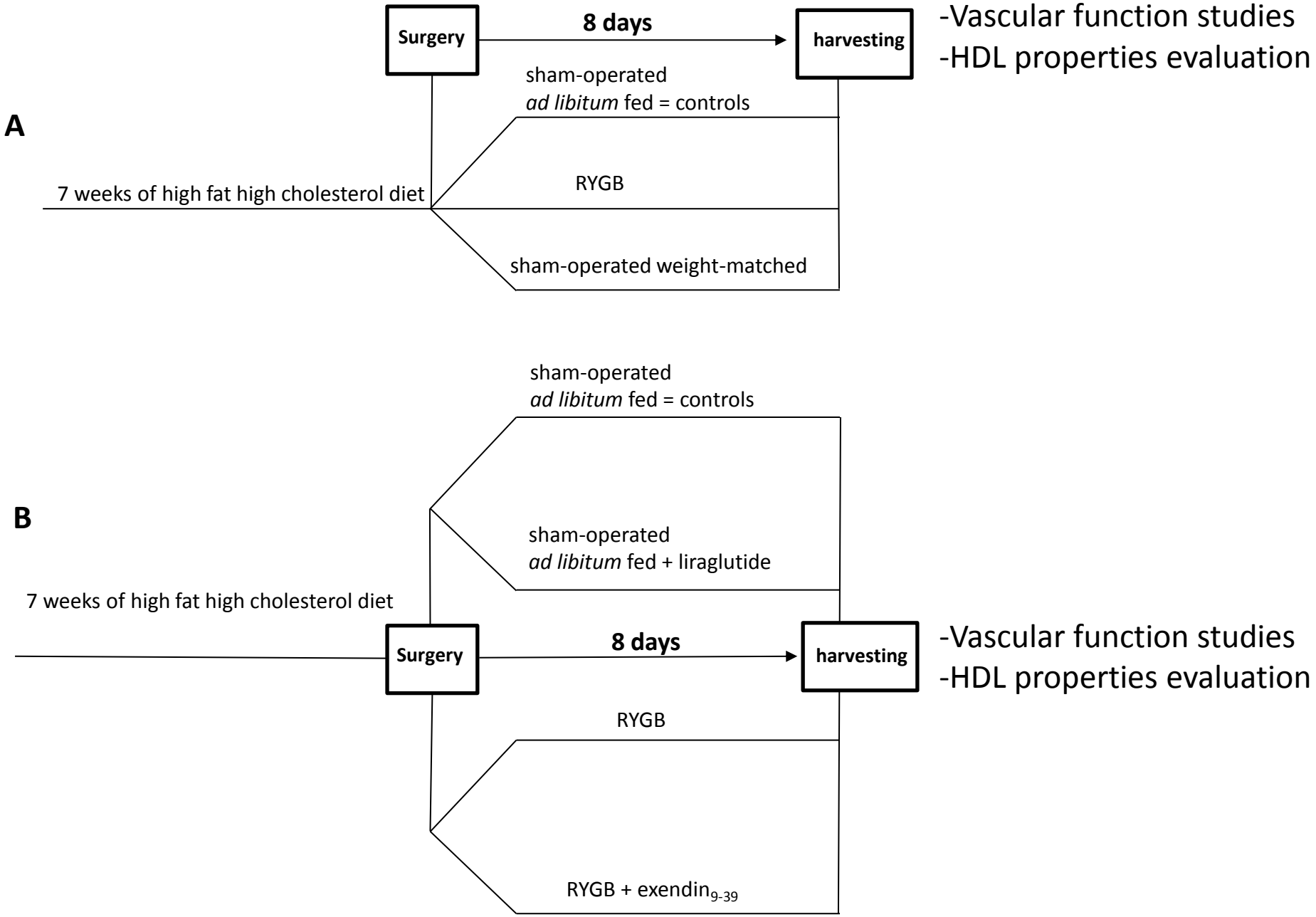
A
Surgery
8 days
harvesting
-Vascular function studies
-HDL properties evaluation
sham-operated
ad libitum fed = controls
7 weeks of high fat high cholesterol diet
RYGB
sham-operated weight-matched
B
sham-operated
ad libitum fed = controls
sham-operated
ad libitum fed + liraglutide
7 weeks of high fat high cholesterol diet
Surgery
8 days
harvesting
-Vascular function studies
-HDL properties evaluation
RYGB
RYGB + exendin$_{9-39}$

SOM Figure 2

A

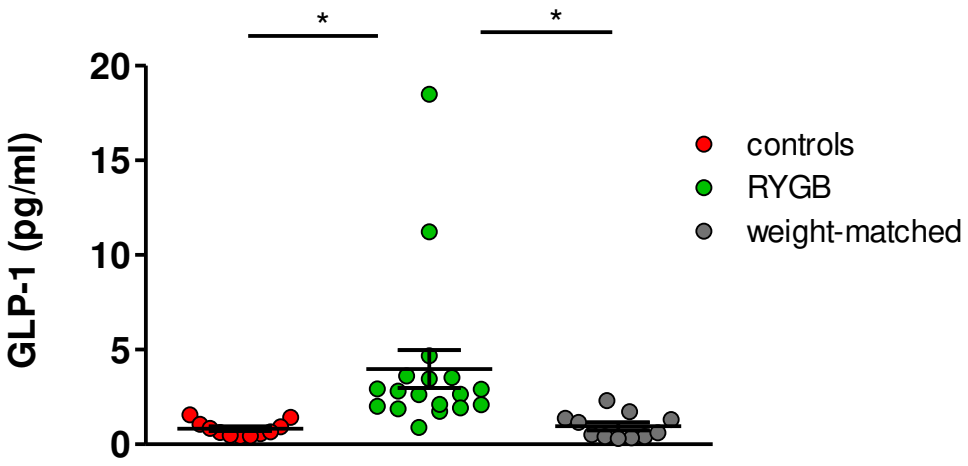

B

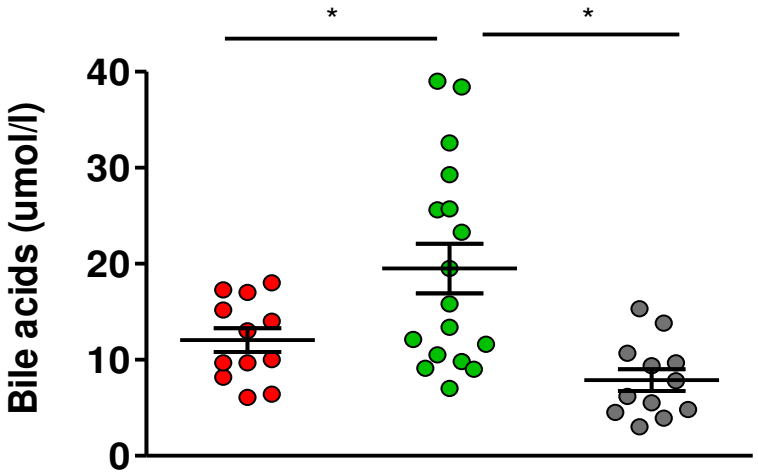

SOM Figure 3

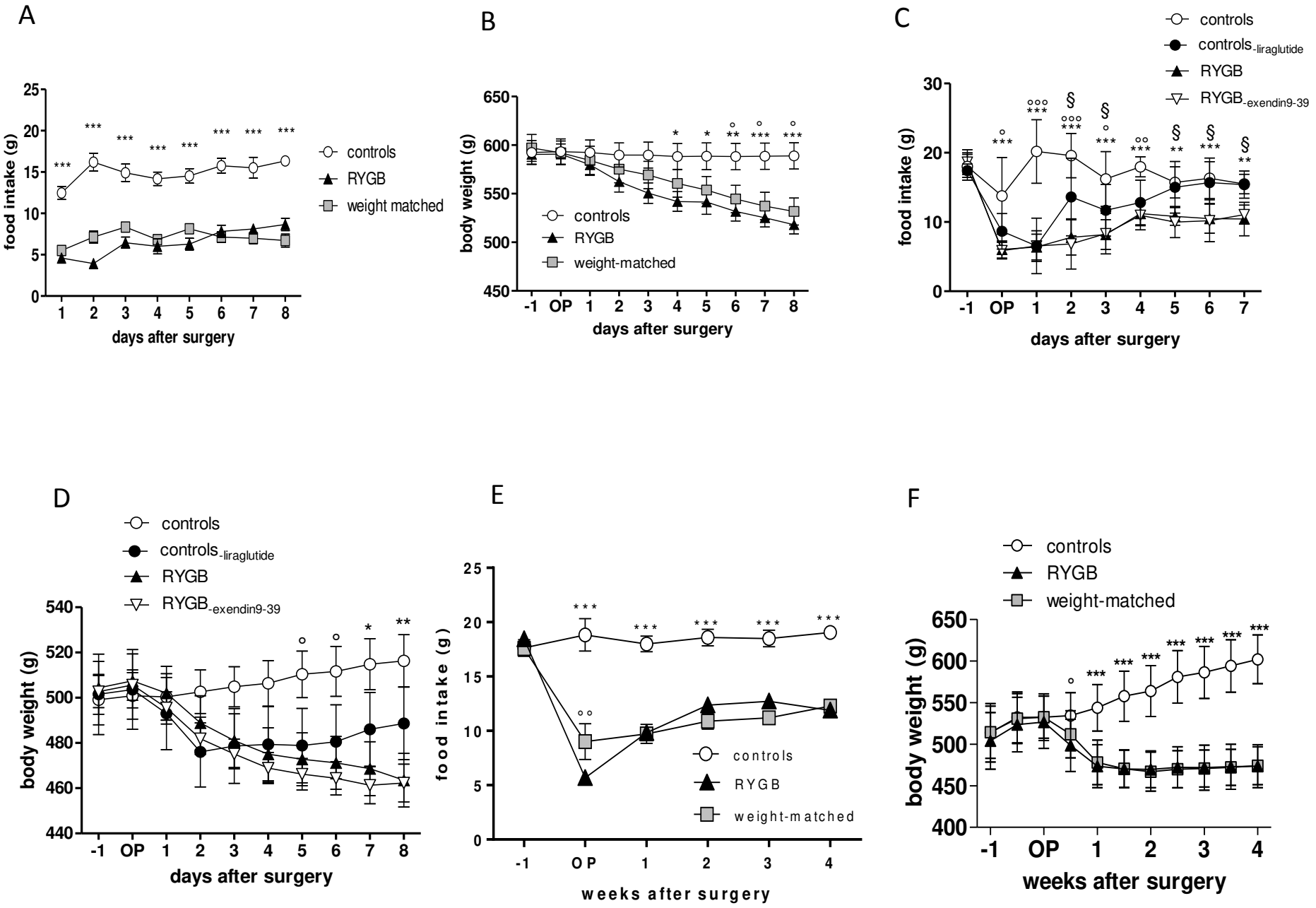
A
food intake (g)
days after surgery
controls
RYGB
weight matched
B
body weight (g)
days after surgery
controls
RYGB
weight-matched
C
food intake (g)
days after surgery
controls
controls-liraglutide
RYGB
RYGB-exendin9-39
D
body weight (g)
days after surgery
controls
controls-liraglutide
RYGB
RYGB-exendin9-39
E
food intake (g)
weeks after surgery
controls
RYGB
weight-matched
F
body weight (g)
weeks after surgery
controls
RYGB
weight-matched

SOM Figure 4

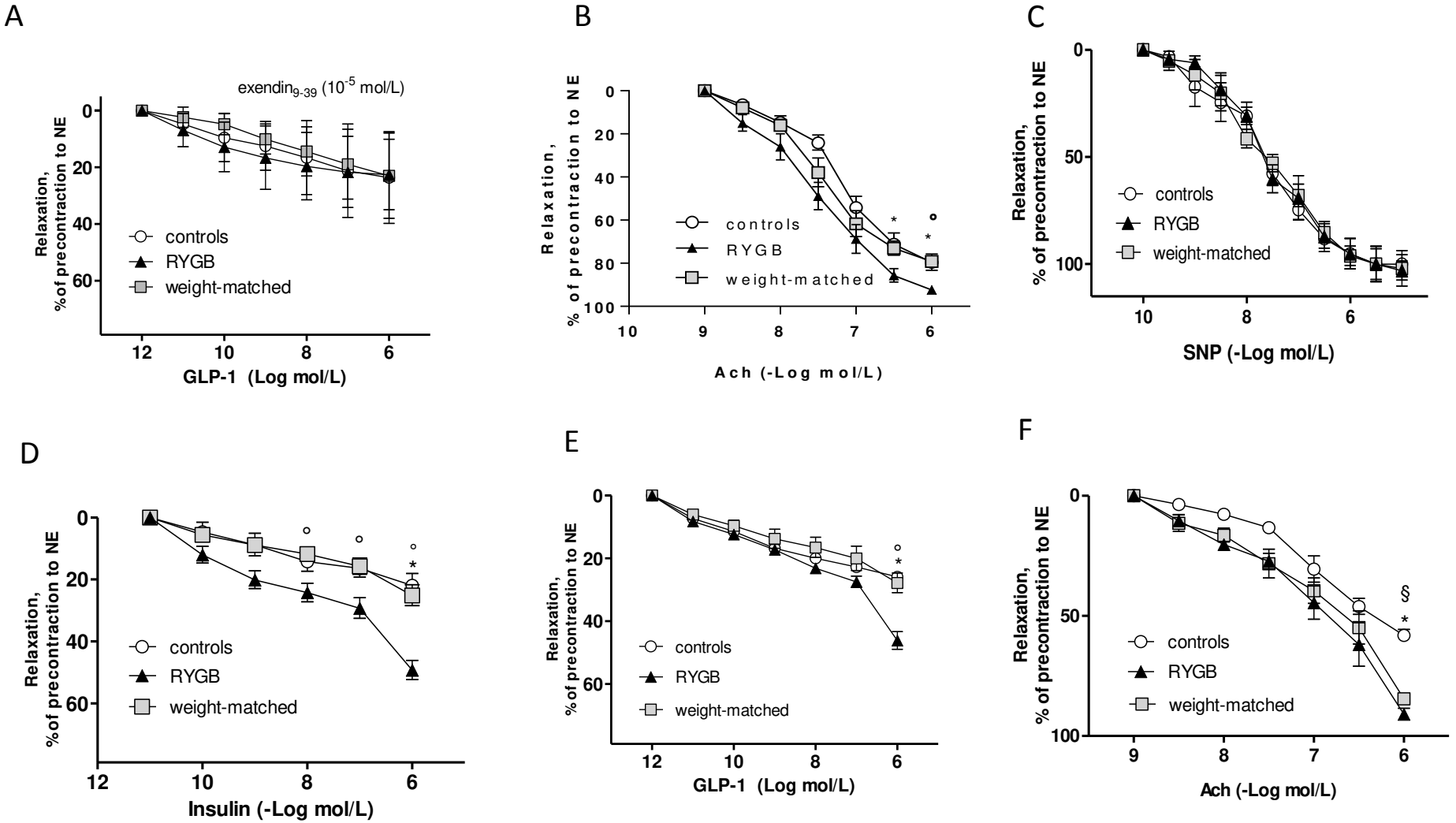
A
exendin9-39 (10-5 mol/L)
Relaxation, %of precontraction to NE
controls
RYGB
weight-matched
GLP-1 (Log mol/L)
B
Relaxation, % of precontraction to NE
Ach (-Log mol/L)
C
SNP (-Log mol/L)
D
Insulin (-Log mol/L)
E
GLP-1 (Log mol/L)
F
Ach (-Log mol/L)

SOM Figure 4

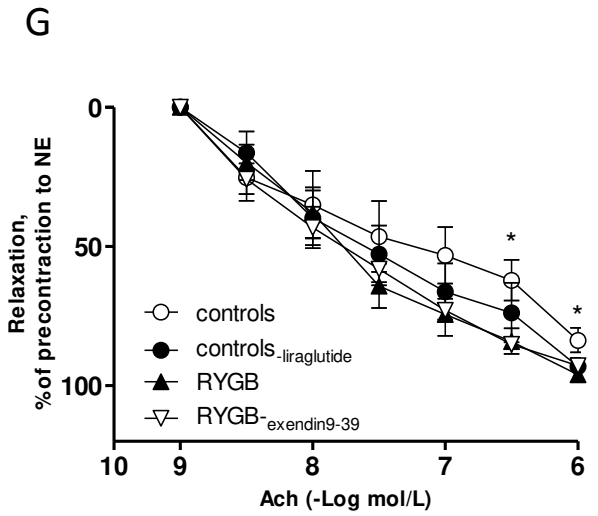
G
Relaxation, %of precontraction to NE
0
50
100
controls
controls-liraglutide
RYGB
RYGB-exendin9-39
10
9
8
7
6
Ach (-Log mol/L)
*
*

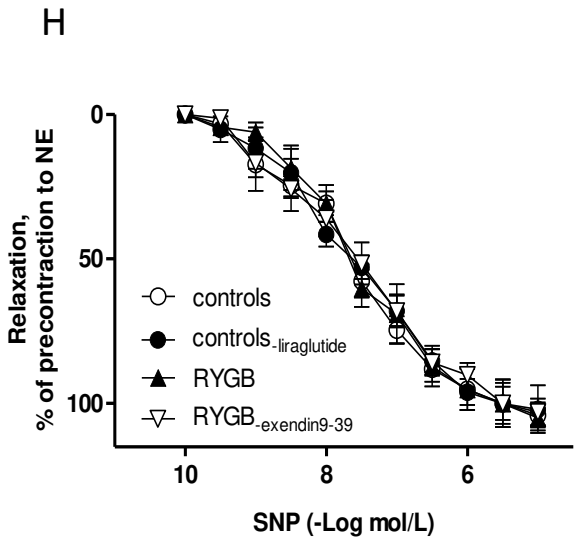
H
Relaxation, % of precontraction to NE
0
50
100
controls
controls-liraglutide
RYGB
RYGB-exendin9-39
10
8
6
SNP (-Log mol/L)

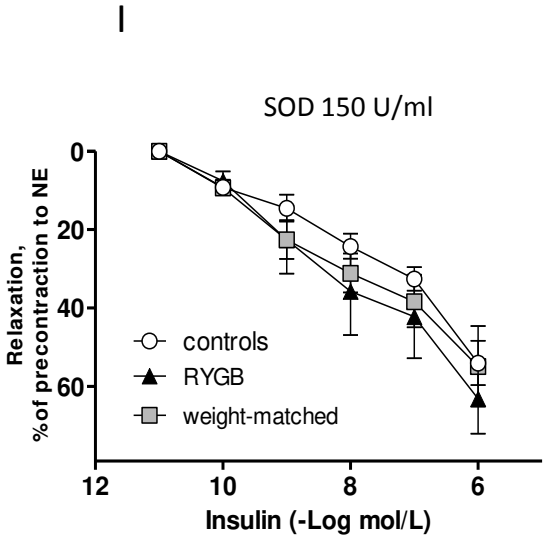
I
SOD 150 U/ml
Relaxation, %of precontraction to NE
0
20
40
60
controls
RYGB
weight-matched
12
10
8
6
Insulin (-Log mol/L)

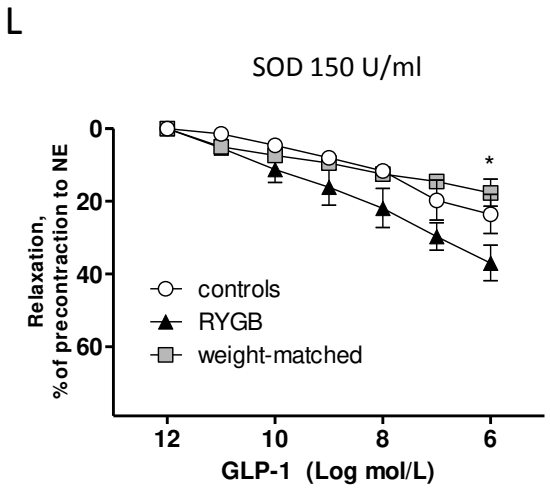
L
SOD 150 U/ml
Relaxation, %of precontraction to NE
0
20
40
60
controls
RYGB
weight-matched
12
10
8
6
GLP-1 (Log mol/L)
*

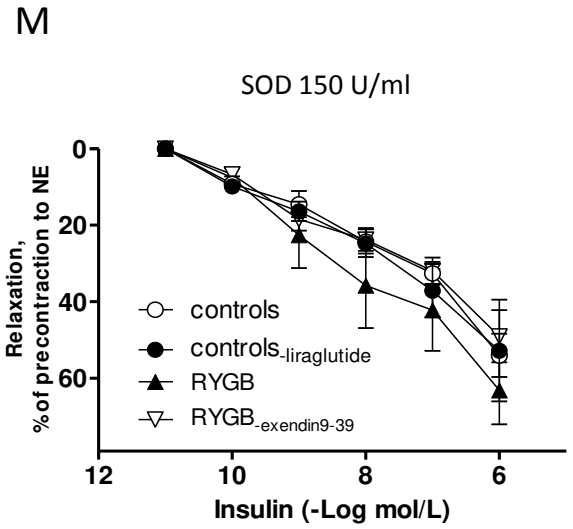
M
SOD 150 U/ml
Relaxation, %of precontraction to NE
0
20
40
60
controls
controls-liraglutide
RYGB
RYGB-exendin9-39
12
10
8
6
Insulin (-Log mol/L)

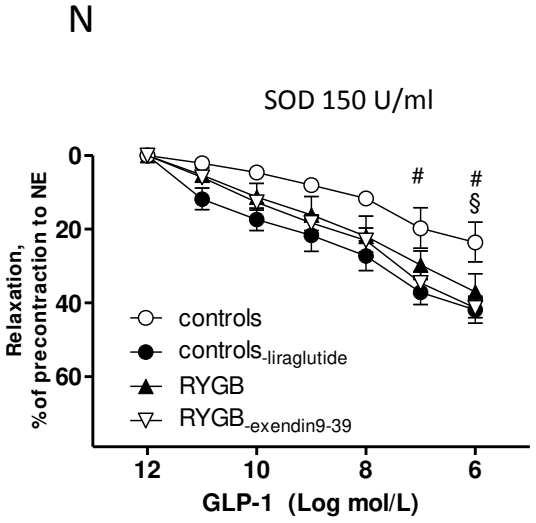
N
SOD 150 U/ml
Relaxation, %of precontraction to NE
0
20
40
60
controls
controls-liraglutide
RYGB
RYGB-exendin9-39
12
10
8
6
GLP-1 (Log mol/L)
#
#
§

SOM Figure 5

A

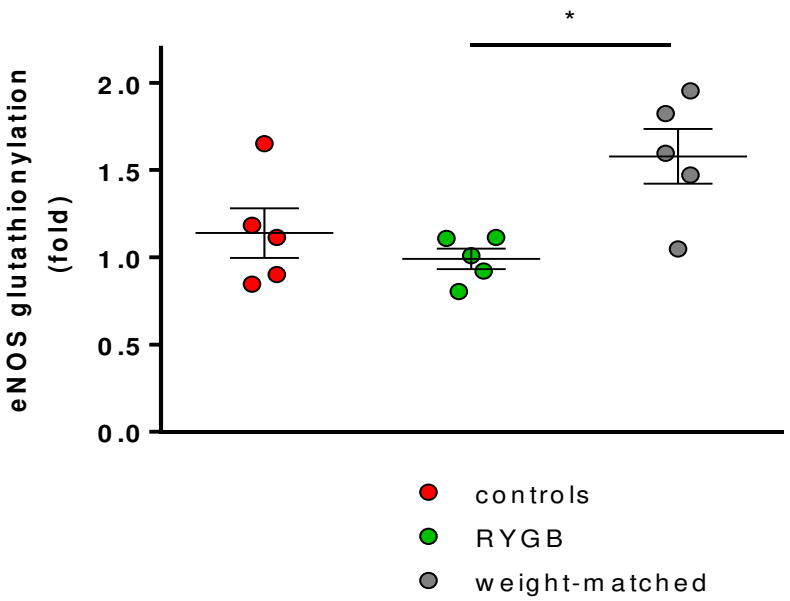

B

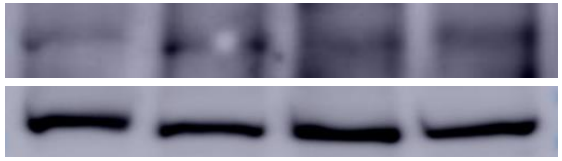

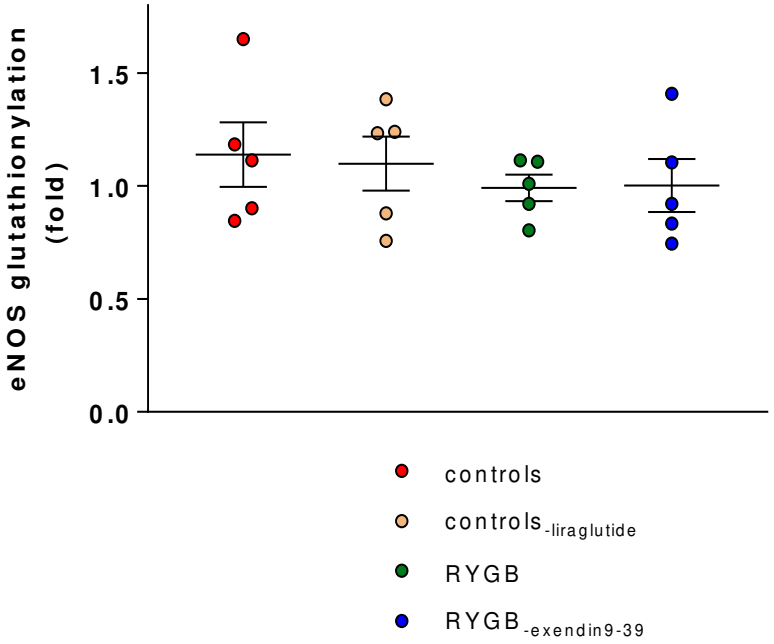

SOM Figure 6

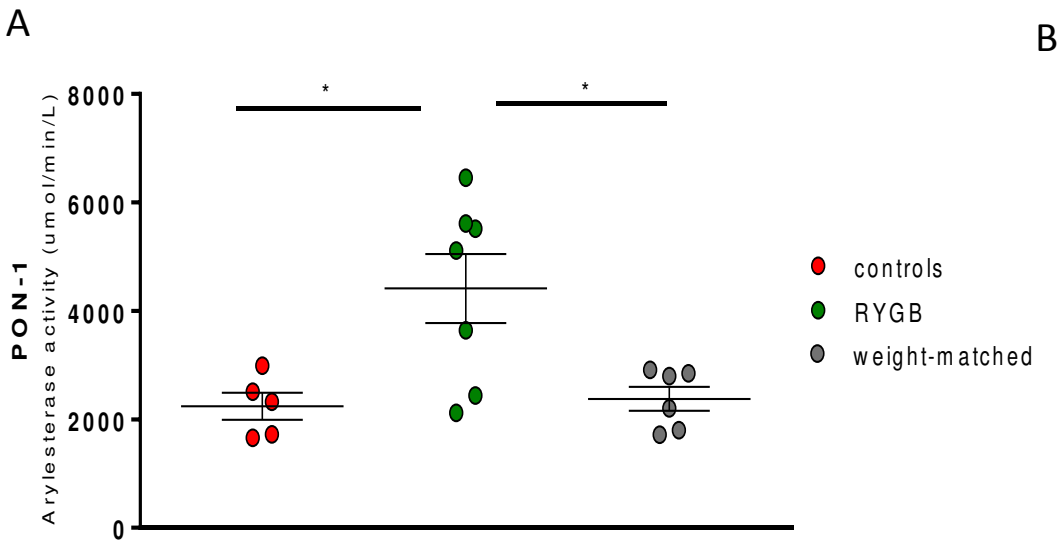
A
PON-1
Arylesterase activity (umol/min/L)
8000
6000
4000
2000
0
*
*
controls
RYGB
weight-matched

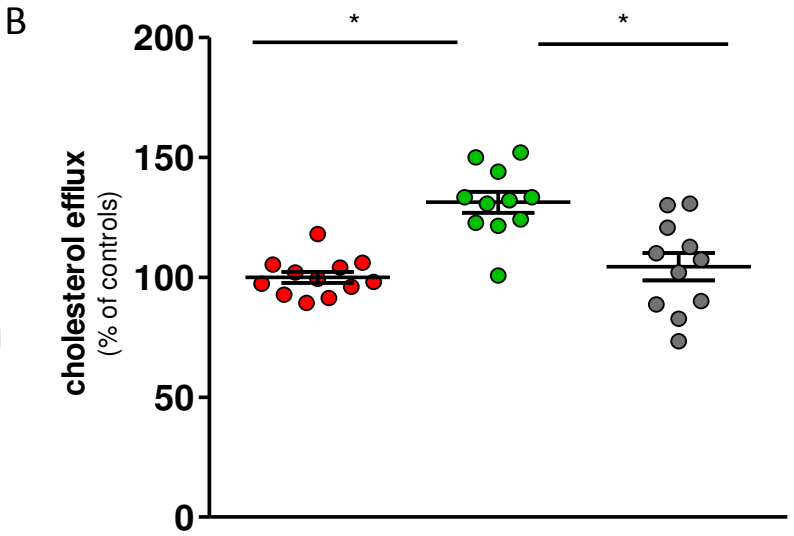
B
cholesterol efflux
(% of controls)
200
150
100
50
0
*
*

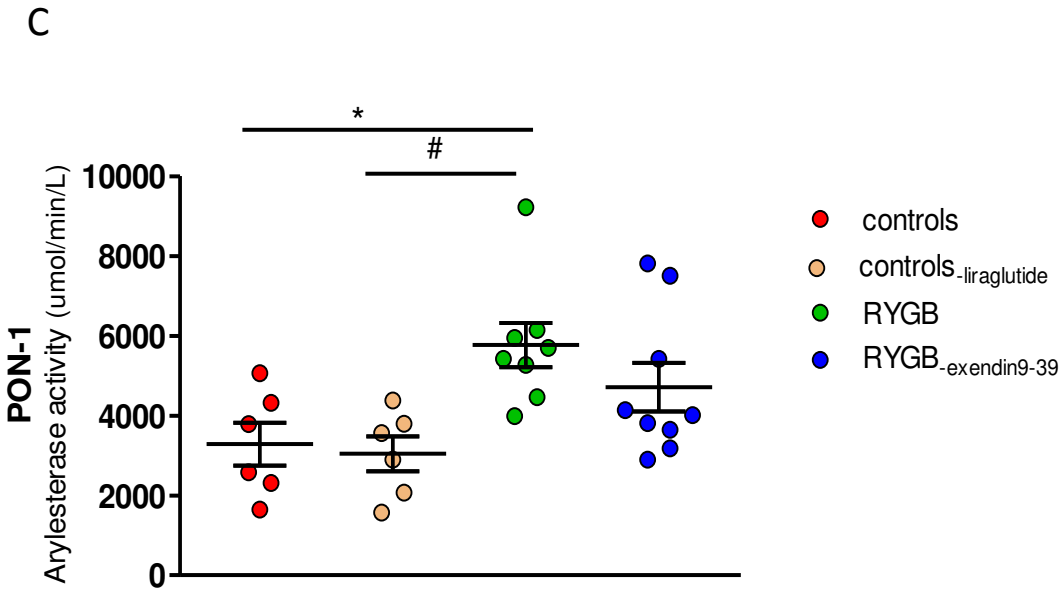
C
PON-1
Arylesterase activity (umol/min/L)
10000
8000
6000
4000
2000
0
*
#
controls
controls-liraglutide
RYGB
RYGB-exendin9-39

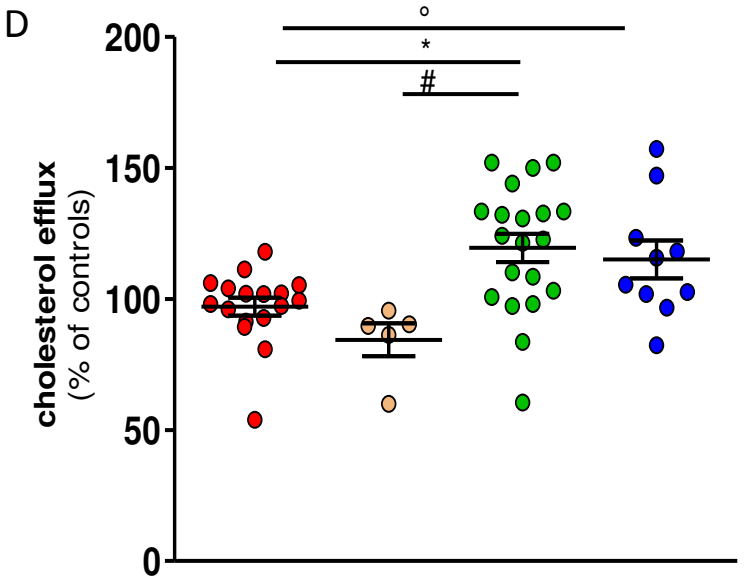
D
cholesterol efflux
(% of controls)
200
150
100
50
0
°
*
#

SOM Figure 7

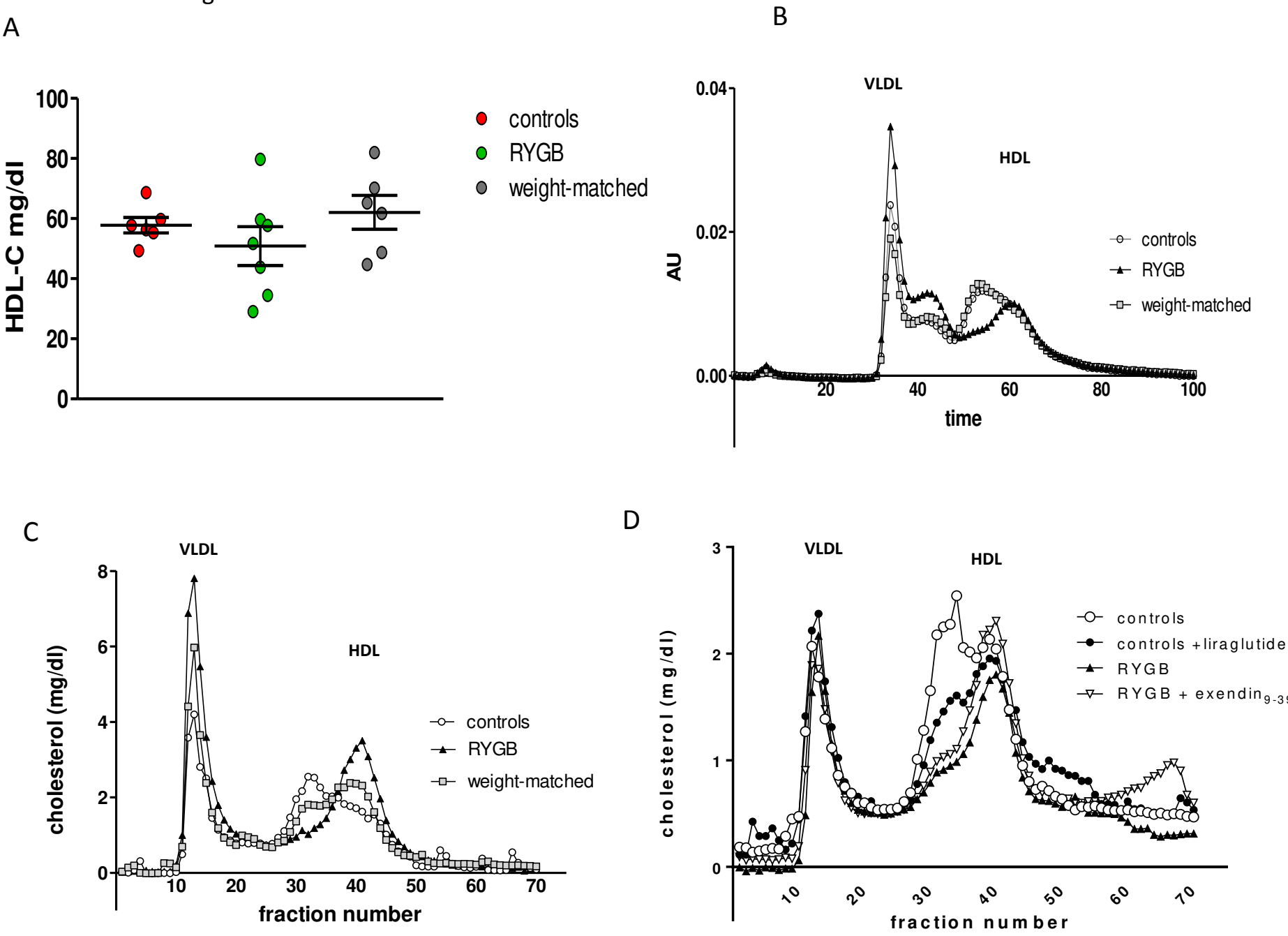
A
HDL-C mg/dl
100
80
60
40
20
0
controls
RYGB
weight-matched
B
VLDL
HDL
0.04
0.02
0.00
AU
20
40
60
80
100
time
controls
RYGB
weight-matched
C
VLDL
HDL
cholesterol (mg/dl)
8
6
4
2
0
10
20
30
40
50
60
70
fraction number
controls
RYGB
weight-matched
D
VLDL
HDL
cholesterol (mg/dl)
3
2
1
0
10
20
30
40
50
60
70
fraction number
controls
controls +liraglutide
RYGB
RYGB + exendin9-39

Table 1: Clinical and Anthropometric Characteristics in Patients and Healthy Subjects

	D0	RYGB D14 (n=29)	12W	BMI-matched to 12W RYGB (n=29)	Healthy (n =28)
Age, years	40.9 ± 1.7			42.7±2.1	37.8±2.4
Female gender, n (%)	17 (58.6%)			19 (65%)	14 (50%)
Height, m	1.7 ± 0.01			1.7± 0.01	1.7± 0.01
Body weight, kg	134.0 ± 3.7[a]	124.0 ± 3.4[ab]	109.3 ± 3.4[ac]	110.3±3.8[abc]	66.0±1.8
BMI (kg/m^2)	45.4 ± 1.0[a]	42.2 ± 1.0[ab]	37.0 ± 1.0[abc]	37.15±0.9[abc]	21.9±0.3
Current smokers (%)	5/29 (17%)	4/29 (14%)	3/29 (10%)	5/29 (17%)	
Diabetes, n (%)	6/29 (20.7%)	4/29 (13.8%)	0/29b (0%)b	2/29 (6.9%)	
OSAS	9/29 (31.0%)	7/29 (24.1%)	6/29 (20.7%)	10/29(34.5%)	
Lipid profile					
Total cholesterol (mmol/l)	4.8 ± 0.2	4.2 ± 0.2[ab]	4.0 ± 0.1[ab]	5.10± 0.20	4.89± 0.10
Log LDL (mmol/l)	1.04 ± 0.05	0.89 ± 0.06[b]	0.85 ± 0.05[b]	1.06± 0.07[bd]	0.98± 0.06
HDL (mmol/l)	0.97(0.82-1.21)	0.77 (0.67-0.97)	0.89 (0.82-1.02)	1.17 (1.01-1.46)[ab]	1.58 (1.29-1.88)
LDL/HDL	3.14±0.23[a]	3.35±0.24[a]	2.70±0.16[abc]	2.65±0.19	1.87±0.19
Log TG (mmol/l)	0.45±0.07[a]	0.53±0.06[a]	0.34±0.04	0.77±0.12[abc]	0.13±0.08
Medications					
Metformin, n (%)	3/29 (10.3%)	2/29 (6.9%)	0/29 (0%)[b]	2/29 (6.9%)	
ACEI (%)	2/29 (6.9%)	2/29 (6.9%)	0/29 (0%)	1/29 (3.4%)	
Sartans	2/29 (6.9%)	2/29 (6.9%)	2/29 (6.9%)	0/29	
B-blockers	5/29 (17.2%)	5/29 (17.2%)	1/29 (3.4%)[b]	0/29	
Statins	0/29 (0%)	0/29 (0%)	0/29 (0%)	6/29 (20.7%)[bcd]	
Ca-channels blockers	2/29 (6.9%)	2/29 (6.9%)	1/29 (3.4%)	0/29	
Diuretics	3/29 (10.3%)	2/29 (6.9%)	1/29 (3.4%)	1/29 (3.4%)	
Others (Gliptins)	1/29 (3.4%)	1/29 (3.4%)	0/29 (0%)	0/29	

Unless specified otherwise, values are means ± SE. Letters indicate statistically significant difference from : (a) Healthy, (b) D0, (c) D14, (d) 12W; (e) BMI-matched to 12W post RYGB; $p<0.05$.
For Log LDL: b vs. c, $p=0.001$; b vs. e, $p<0.0001$; d vs. e, $p=0.03$.
For HDL: $p<0.0001$ except for b vs. e, $p=0.01$
For Log TG: $p<0.0001$ except for c vs. e, $p=0.002$; b vs. e, $p=0.03$ and d vs. e, $p=0.003$.

BMI, body mass index. OSAS, obstructive sleep apnea syndrome. LDL, low density lipoprotein. HDL, high density lipoprotein. TG, triglycerides. ACEI, Angiotensin-converting-enzyme inhibitors.

Table 2: GLP-1, bile acids and glycemic profile in Patients and Healthy Subjects

	RYGB			BMI-matched to 12W RYGB	Healthy
	D0	D14	W12	(n=29)	(n =28)
		(n=29)			
Log GLP-1, pg/ml	-0.76±0.2[a]	0.69±0.1[b]	0.40±0.1[b]		0.29±0.13
Log Bile acids, umol/L	2.02±0.06[a]	2.19±0.05[ab]	2.39±0.06[bc]		2.4±0.06
Glucose, mmol/L	6.40±0.25[a]	5.39±0.11[b]	5.12±0.11[b]	5.49±0.27	5.29±0.15
Log Insulin, UI/ml	2.69±0.16[a]	2.49±0.09[ab]	2.28±0.1[b]	2.41±0.113[ac]	1.58±0.16
Log HOMA IR	0.69±0.15[a]	0.48±0.09[ab]	0.20±0.11[abc]	0.37±0.13[a]	-0.42±0.16

Unless specified otherwise, values are means ± SE. Letters indicate statistically significant difference from : (a) Healthy, (b) D0, (c) D14, (d) 12W, (e) BMI-matched to 12W post RYGB; $p<0.05$.
For Log GLP-1: $p<0.0001$.
For Log Bile acids: $p <0.0001$; except c vs. d, $p< 0.01$.
For Glucose: b vs. d 0.002
For Log Insulin: $p<0.0001$; except: c vs. d, $p< 0.03$; a vs. e, $p< 0.001$
Log HOMA IR: $p<0.0001$; except: b vs. d, $p< 0.01$; c vs. d, $p< 0.004$; a vs. d 0.004.

GLP-1, Glucagon-like peptide-1. HOMA IR, Homeostatic model assessment for insulin resistance.

Table 3. Overwiev of the RYGB-specific, weight-independent and GLP-1-mediated rapid effects on endothelial–mediated relaxation and HDL vaso-protective properties

	Rats eight days after RYGB			Patients after RYGB
	Improved after RYGB and weight-independent*	Improved by liraglutide in sham-operated controls†	Blocked by exendin$_{9-39}$ in RYGB‡	
Vasorelaxation in response to:				
Insulin	**YES**	**YES**	**YES**	
GLP-1	**YES**	**YES**	**YES**	
Acetylcholine	**YES**	**YES**		
HDL- mediated vaso-protective properties:				
NO production	**YES**	**YES**		**YES §**
Anti-apoptosis	**YES**	**YES**		**YES**
Anti-inflammatory	**YES**	**YES**		**YES §**
Anti-oxidant (NADPH oxidase activity)	**YES**	**YES**		**YES §**
PON-1 activity	**YES**			**YES §**
Cholesterol efflux	**YES**			**YES §**

*weight-independent effects are considered effects observed in RYGB but not in sham-operated weight-matched rats.

†Improved by liraglutide suggests effects involving GLP-1 activated signaling.

‡ Blocked by exendin$_{9-39}$ suggests effects mediated by the classical GLP-1 receptor.

§ protective HDL properties observed in patients 12 weeks after RYGB but not in the BMI-matched patients.